
















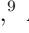



Searching for electromagnetic emission in an AGN from the gravitational wave binary black hole merger candidate S230922g^{*†}

TOMÁS CABRERA ¹, ANTONELLA PALMESE ¹, LEI HU ¹, BRENDAN O’CONNOR ^{1,‡}, K.E.SAAVIK FORD ^{2,3,4},
BARRY MCKERNAN ^{2,3,4}, IGOR ANDREONI ^{5,6,7}, TOMÁS AHUMADA ⁸, ARIEL AMSELLEM ¹, MALTE BUSMANN ⁹,
PETER CLARK ¹⁰, MICHAEL W. COUGHLIN ¹¹, EKATERINE DADIANI ¹, VERONICA DIAZ ¹, MATTHEW J. GRAHAM ⁸,
DANIEL GRUEN ^{9,12}, KEERTHI KUNNUMKAI ¹, JAKE POSTIGLIONE ⁴, JULIAN S. SOMMER ⁹ AND
FRANCISCO VALDES ¹³

- ¹ *McWilliams Center for Cosmology and Astrophysics, Department of Physics, Carnegie Mellon University, 5000 Forbes Avenue, Pittsburgh, PA 15213*
² *Center for Computational Astrophysics, Flatiron Institute, 162 5th Ave, New York, NY 10010, USA*
³ *Department of Astrophysics, American Museum of Natural History, New York, NY 10024, USA*
⁴ *Department of Science, BMCC, City University of New York, New York, NY 10007, USA*
⁵ *Joint Space-Science Institute, University of Maryland, College Park, MD 20742, USA*
⁶ *Department of Astronomy, University of Maryland, College Park, MD 20742, USA*
⁷ *Astrophysics Science Division, NASA Goddard Space Flight Center, Mail Code 661, Greenbelt, MD 20771, USA*
⁸ *Division of Physics, Mathematics, and Astronomy, California Institute of Technology, Pasadena, CA 91125, USA*
⁹ *University Observatory, Faculty of Physics, Ludwig-Maximilians-Universität München, Scheinerstr. 1, 81679 Munich, Germany*
¹⁰ *Institute of Cosmology and Gravitation, University of Portsmouth, Portsmouth, PO1 3FX, UK*
¹¹ *School of Physics and Astronomy, University of Minnesota, Minneapolis, Minnesota 55455, USA*
¹² *Excellence Cluster ORIGINS, Boltzmannstr. 2, 85748 Garching, Germany*
¹³ *NSF National Optical-Infrared Research Laboratory, 950 N. Cherry Ave., Tucson, AZ 85719, USA*

ABSTRACT

We carried out long-term monitoring of the LIGO/Virgo/KAGRA binary black hole (BBH) merger candidate S230922g in search of electromagnetic emission from the interaction of the merger remnant with an embedding active galactic nuclei (AGN) accretion disk. Using a dataset primarily composed of wide-field imaging from the Dark Energy Camera (DECam) and supplemented by additional photometric and spectroscopic resources, we searched $\sim 70\%$ of the sky area probability for transient phenomena, and discovered 6 counterpart candidates. One especially promising candidate - AT 2023aagj - exhibited temporally varying asymmetric components in spectral broad line regions, a feature potentially indicative of an off-center event such as a BBH merger. This represents the first *live* search and multiwavelength, photometric, and spectroscopic monitoring of a GW BBH optical counterpart candidate in the disk of an AGN.

1. INTRODUCTION

As multimessenger astronomy continues to develop, the branch of this field dedicated to studying **compact binary coalescences (CBCs)** stands as an important forerunner as the first to include direct observations of **gravitational waves (GWs)** (Abbott et al. 2017a). These events manifest phenomena at scales presently unobtainable in man-made environments, and hence are important natural laboratories in which to study extreme physics such as heavy element nucleosynthesis (Symbalysty & Schramm 1982) and measure key physical quantities such as the expansion rate of the universe (Schutz 1986; Holz & Hughes 2005).

This potential was realized following the first successful multimessenger detection of the binary neutron

Corresponding author: Tomás Cabrera
tcabrera@andrew.cmu.edu

^{*} based on observations made with the Southern African Large Telescope (SALT)

[†] Some of the data presented herein were obtained at Keck Observatory, which is a private 501(c)3 non-profit organization operated as a scientific partnership among the California Institute of Technology, the University of California, and the National Aeronautics and Space Administration. The Observatory was made possible by the generous financial support of the W. M. Keck Foundation.

[‡] McWilliams Fellow

star merger GW170817/GRB 170817A (Abbott et al. 2017b), wherein a global electromagnetic astronomy campaign succeeded in locating a kilonova (KN) (Coulter et al. 2017; Arcavi et al. 2017; Andreoni et al. 2017; Drout et al. 2017; Nicholl et al. 2017; Evans et al. 2017; Lipunov et al. 2017; Pian et al. 2017; Smartt et al. 2017; Utsumi et al. 2017; Valenti et al. 2017; Kasliwal et al. 2017; Troja et al. 2017; Margutti et al. 2017; Shappee et al. 2017; Soares-Santos et al. 2017; Chornock et al. 2017; Tanvir et al. 2017) incident with the initially identified GW and gamma ray burst (GRB) events (Abbott et al. 2017a; Savchenko et al. 2017; Goldstein et al. 2017). This single event by itself was enough to result in hundreds of analyses, including constraints on neutron star (NS) physics (e.g. Abbott et al. 2018) and the Hubble constant H_0 (Abbott et al. 2017c). In the case of H_0 , it is predicted that $\mathcal{O}(100)$ binary neutron star (BNS) events with electromagnetic (EM) counterparts are required to make a \sim few% measurement of the parameter (Chen et al. 2018), although joint multimessenger constraints on the binary viewing angle can further improve precision by a factor of a few (e.g. Hotokezaka et al. 2019; Palmese et al. 2024).

While BNS mergers are the only class of GW event with a confirmed EM counterpart, it is also predicted that binary black hole (BBH) mergers can produce counterparts in certain circumstances. The majority of proposed counterpart mechanisms involve the interaction of the binary or merger remnant with a coexistent medium, usually the gaseous accretion disk of an active galactic nucleus (AGN), whether through accretion (Bartos et al. 2017b), ram-pressure stripping of gas about the remnant or jetted Bondi accretion (McKernan et al. 2019), or breakout emission from a post-merger jet (Tagawa et al. 2023; Tagawa et al. 2024). A cartoon of the AGN-associated EM counterpart mechanism is shown in Figure 1.

Counterpart candidates for BBH mergers from previous LIGO/Virgo/KAGRA (LVK) observing runs have been proposed (Graham et al. 2020, 2023), although confirmation of a counterpart has remained challenging. There are several reasons for this difficulty. First, even if we know that a given merger happens in an AGN, in principle there is only a $\mathcal{O}(1/4)$ chance that we could detect an EM counterpart: our view of around half of AGN (the Type 2s) is obscured, and an unfortunate kick-direction out the opposite side of a Type 1 AGN could still obscure any emission (Graham et al. 2023). Second, even if a flare emerges from an AGN, it must be discerned in the presence of other AGN variability. This makes our task of searching for counterparts more challenging in brighter AGN, and our search is biased

against less luminous counterparts. Third, possible flare parameters are weakly constrained, both because AGN disk properties are uncertain to orders of magnitude, and because the properties of the post-merger flare depend on these uncertain parameters.

One possible means to confirm a counterpart is through optical spectroscopy: because the BBH merger occurs off-center in the AGN disk, the resulting flare could unevenly illuminate the broad-line region (BLR) of the AGN, resulting in asymmetric broad-line features in the optical spectrum (McKernan et al. 2019). Synchronized evolution of a transient with such spectral features can be a key piece of evidence in favor of the classification of a transient as a EM counterpart to a BBH merger. At the very least, an evolving asymmetric line profile suggests an off-center flaring event in the AGN, ruling out most sources of AGN variability near the SMBH. Flare energetics and lightcurve profiles can allow us to rule out e.g. embedded supernovae, leaving few candidates for a sufficiently energetic off-center AGN flare, including a BBH merger.

Certainly, the search for EM counterparts to BBH mergers has unique challenges versus the search for NS merger counterparts (intrinsic AGN variability, delay time uncertainties, etc.); however, as the historical rate of detection of BBH mergers has been $\sim \mathcal{O}(100) \times$ greater than that for NS mergers, there are many more opportunities to search for a counterpart to the former kind of event. Because multimessenger observations of BBH mergers are also useful in making cosmological measurements (Palmese et al. 2021; Bom & Palmese 2023; Alves et al. 2024), the pursuit of EM counterparts to BBH mergers has the potential to significantly contribute to the multimessenger observations required to make the first 2% measurement of the Hubble constant with standard sirens, which the level of precision needed to help us understand the Hubble tension (Chen et al. 2018).

Currently, GW follow-up of distant events is best enabled with technology capable of meeting the colloquial requirements of “wide, fast, deep”, as to ensure the rapid and thorough coverage of event volumes. The Dark Energy Camera (DECam) (Flaugher et al. 2015) on the 4m Victor M. Blanco Telescope at the Cerro Tololo Inter-American Observatory (CTIO) is one of the premiere instruments that can address these requirements. DECam already has a respectable history in GW follow-up, having been used for this purpose from the first GW event (Soares-Santos et al. 2016; Annis et al. 2016) and many events since then (Goldstein et al. 2019; Andreoni et al. 2019; Herner et al. 2020; Andreoni et al. 2020; Morgan et al. 2020; Garcia et al. 2020), and importantly

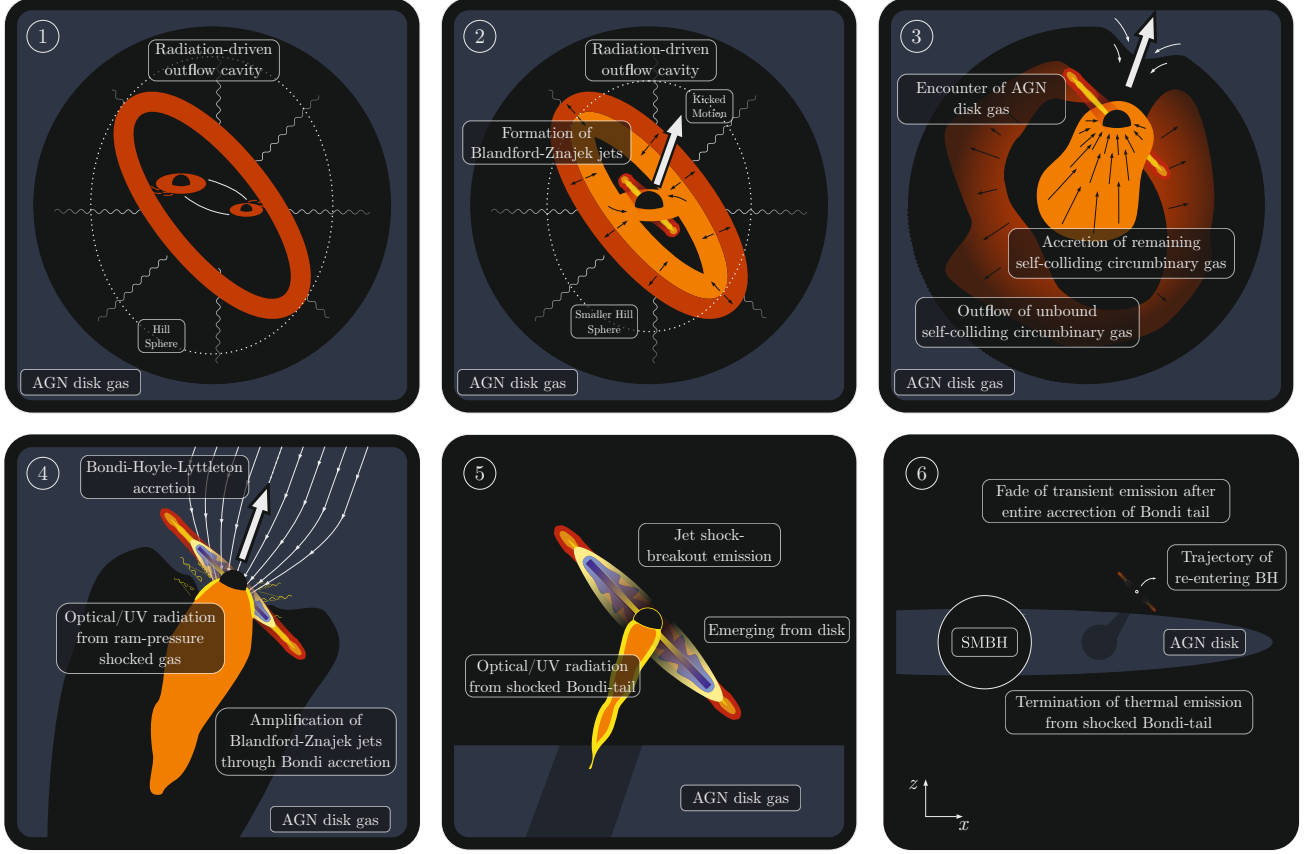


Figure 1. Multi-panel schematic showing the mechanism believed to underpin luminous EM counterparts to BBH mergers in AGN disks. In panel 1, the pre-merger BH accretes from mini-disks within its Hill sphere in the AGN disk midplane and blows a cocoon within the disk via feedback. In panel 2, the merger happens, forming a highly spinning BH (dimensionless spin parameter $a \sim 0.7$ typically). A jet is presumed to form at this stage (although it has yet to be established whether such a jet can persist for long, or whether it is choked off by high mass accretion). Mass and spin asymmetries in the progenitor black holes lead to a kick at merger (depicted by the arrow in panel 2). Panels 3 and 4 show the development of BHL accretion as the newly merged BH exits its original Hill sphere into the rest of the AGN disk, powering a luminous transient. In panel 5 the BH emerges from the AGN disk, dragging disk gas with it. In panel 6 the EM emission fades as the disk material is consumed and the BH continues on an inclined orbit around the SMBH, and will re-enter the AGN disk on half the orbital timescale.

being one of the first instruments to detect the counterpart KN to GW170817 (Soares-Santos et al. 2017). The new survey program Gravitational Wave MultiMessenger Astronomy DECAM Survey (GW-MMADS) (PIs: Andreoni & Palmese) is designed to find EM counterparts to BNS, NSBH, and BBH mergers via rapid DECAM follow-up of GW events during the fourth gravitational wave observing run (O4).

In this work, we present results from our follow up of the GW event S230922g. S230922g is a LVK BBH merger candidate detected at 2023-09-22 02:03:44.886 UTC (Ligo Scientific Collaboration et al. 2023a,b). The 90% credible region of 324 deg^2 is one of the smallest areas of O4a (the first part of O4, completed in January 2024); this, combined with the localization being visible from Chile in the months following the trigger, made an

effective follow-up with DECAM possible in pursuit of potential AGN-linked counterparts like those mentioned previously. In this paper we present our long-term monitoring of S230922g; the paper is organized as follows: §2 presents our program’s generic strategy for GW follow-up and the data collected, highlighting components especially relevant for S230922g; §3 describes the methods we used to distill our population of detected transients into a shortlist of counterpart candidates; §4 describes our most favored candidate, and to a lesser extent additional candidates of interest; in §5 we estimate parameters for our most favored counterpart candidate, finding it well within the confines of existing BBH counterpart theory; in §6 we summarize our findings and highlight considerations relevant for future efforts. Throughout

this work we use a flat Λ CDM model with $H_0 = 70$ km/s/Mpc and matter density of $\Omega_m = 0.3$,

2. DATA

2.1. GW data

S230922g is an event of interest because it was detected with high significance (False Alarm Rate - FAR - 1 per 1.6×10^{-16} years from `gstlal`; Messick et al. 2017; Sachdev et al. 2019) by both LIGO Livingston and LIGO Hanford, it is well localized compared to the O4a population, and it has $\sim 100\%$ probability of being a BBH. It was also identified with high significance by the Burst CWB (Klimenko et al. 2016) search pipeline, potentially indicating a loud, short burst, as one may expect for a massive BBH spending a short fraction of the late inspiral phase in the LVK band. The luminosity distance of the event, marginalized over the entire sky, is $d_L = 1491 \pm 443$ Mpc. These quantities are reported with the skymap from the Bilby (Ashton et al. 2019) reduction (LIGO Scientific Collaboration et al. 2023c); we use this skymap for our work.

Higher mass ($M_{\text{tot}} \gtrsim 50 M_\odot$) BBH mergers are more likely to have originated from the disks of AGNs (e.g. Gayathri et al. 2021), and so we also inform our decision to trigger BBH follow up by estimating the total mass of the binary. We follow a similar calculation to that in Graham et al. (2020), and consider that $A_{90} \propto \text{SNR}^{-2}$ (Berry et al. 2015), as well as $\text{SNR} \propto \mathcal{M}_c^{5/6}/d_L$ (Finn & Chernoff 1993), where \mathcal{M}_c is the chirp mass of the binary. For this event, we assume a 1.4-1.4 M_\odot binary neutron star merger detection horizon of 150 and 152 Mpc for Hanford and Livingston, respectively, an equal mass system, and the luminosity distance marginalized over the sky; we derive a total rest frame mass of $M_{\text{tot}} \sim 90 M_\odot$ for S230922g. Note that this estimate is highly uncertain with an error bar of at least a factor of 2.

2.2. DECam observations

Our team was notified of S230922g through a General Coordinates Network (GCN) listener¹ that sent a digest of the event to our Slack workspace.² Our first response was to generate an initial observing strategy with `gwemopt` (Coughlin et al. 2018) to assess the probability coverage possible with a single night of DECam observations. `gwemopt` selects exposure pointings from a pre-set sky tiling. Because our image subtraction pipeline

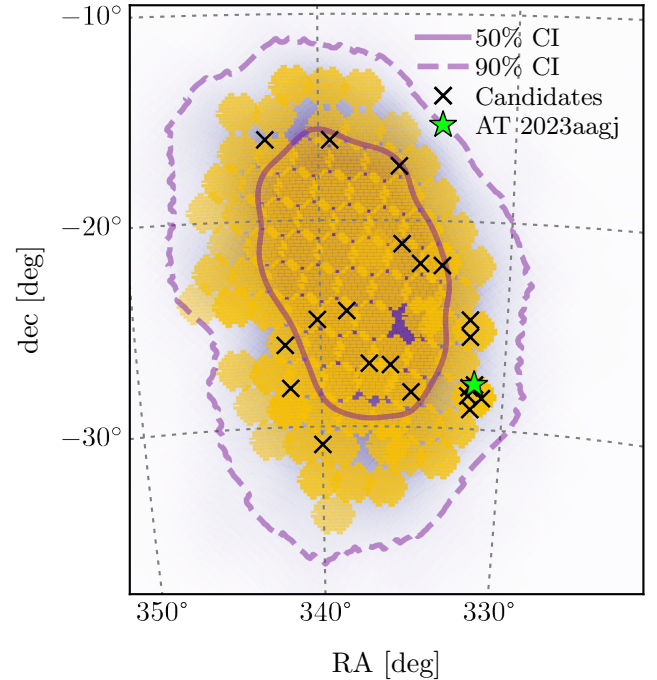


Figure 2. Our observation plan for follow up of S230922g. The LVK skymap for the event is plotted on the lower layers of the figure, and the 50% (90%) credible interval regions are outlined in the solid (dashed) line. The candidates composing our shortlist are shown as black X's, with our favored candidate indicated with a green star.

uses archival DECam exposures as templates, we implemented a custom tiling based on images calibrated by the NSF National Optical-Infrared Research Laboratory (NOIRLab) DECam Community Pipeline (CP) (Valdes et al. 2014) and made available through the NOIRLab Astro Data Archive³ (McManus & Olsen 2021) to ensure our observing plans include pointings with usable templates. During each observing night, the CP calibrates the response and astrometry of each exposure shortly after it is taken which is then available to the image subtraction pipeline.

We determined that 70% of the GW localization area could be covered with 60s and 80s DECam exposures in *g*- and *i*-bands, respectively, with ~ 4.7 hours of telescope time. Our DECam tiling is shown in Figure 2, overlaid on the LVK Bilby skymap (LIGO Scientific Collaboration et al. 2023b) for S230922g. When this plan was finalized, we communicated our pointings to the larger astronomical community through the GW Trea-

¹ Adapted from <https://github.com/scimma/slackbot>.

² Our team also uses the Fritz science data platform (Coughlin et al. 2023) for notifications of GW events via phone call, but we reserve this kind of notification for exceptionally time-sensitive events such as BNS and NSBH mergers.

³ <https://astroarchive.noirlab.edu/>

sure Map⁴ (Wyatt et al. 2020), and we updated information appropriately as we executed our plan.

Leading BBH counterpart models predict delays of 1-3 weeks after the merger before the manifestation of any EM counterpart, due to the need for the signal to first emerge from the depths of the AGN disk. Even so, it is valuable to initiate EM follow up for these kinds of events within a few days of the GW trigger, as high-cadence archival data are generally not available in the localization area of a given GW event and a baseline of sources in the localization area can be useful when vetting candidates. Accordingly, we decided to trigger our Target of Opportunity (ToO) program for the night following the event (the evening of September 22, 2023) in order to establish a baseline of activity at the GW merger time and to facilitate the identification of novel phenomena in subsequent observing epochs.

On the first night we were only able to complete ~ 1 hour of observations before inclement weather began, but we were able to observe our full plan in its entirety the following night (September 23). We publicly reported transients in the area through GCN within 24 hours of these observations (Cabrera et al. 2023). Further observations were conducted 11, 33, 41, and 70 days after the LVK trigger (October 3, October 25, November 2, and December 1). As we processed the data throughout the campaign, we took additional observations of the most interesting candidates, adding up to eight epochs altogether. We submitted all transient sources discovered through this campaign to the Fritz SkyPortal (van der Walt et al. 2019; Coughlin et al. 2023). After composing our final candidate shortlist (as detailed in §3), we reported the respective sources to the Transient Name Server (TNS).

2.3. Spectroscopic observations

BBH counterpart models have some degeneracy with those for stochastic AGN variability and other transient events like tidal disruption events (TDEs), but spectroscopic data has been predicted to serve as a key discriminator among these phenomena: specifically, the off-center location of a BBH merger in the accretion disk of the AGN as opposed to the central location of TDEs or accretion-based phenomena is expected to induce asymmetry in the broad lines of AGN spectra as the transient event “washes” over the BLR in an asymmetric manner (McKernan et al. 2019). The detection of a BLR asymmetry that evolves in concert with the light curve of a transient is a smoking gun that locates the transient in

Table 1. Summary of selection cuts applied to our pipeline products. The table is split into two sections: cuts applied to individual difference image detections (first 3 cuts), and those applied to multi-epoch light curves composed of coincident detections (remaining 6 cuts).

Vetting filter	# passed	Frac. passed
<i>Detection-based cuts</i>		
Initial photometry detections	25,392,140	1.00
Data quality masking	14,053,259	0.553
Real/bogus score ≥ 0.7	1,501,800	0.059
<i>Source-based cuts</i>		
Initial transients	233,313	1.00
Remove LS variable stars	140,230	0.601
Remove MPC objects	18,528	0.079
≥ 1 real/bogus score ≥ 0.9	17,515	0.075
≥ 2 detections with $\Delta t \geq 30$ min	3558	0.015
LS galaxy sep $\leq 1''$	2388	0.010
Additional vetting	6	2.6e-5

an off-center position in the accretion disk expected for BBH mergers, and the coincidence of such an event with a GW merger is a strong evidence standard astronomical techniques can provide linking BBH mergers and AGN flares.

In pursuit of such evidence, we triggered several spectroscopic resources for additional follow-up of transients whose light curves demonstrated proposed counterpart features (see §3.1). A total of five spectra were collected during our follow-up campaign: two with Gemini GMOS, and one each with Keck LRIS, SALT RSS, and P200 DBSP. We discuss the methodology for each spectrum in the context of the respective candidate in §4.2.

3. METHODS

3.1. Automated vetting

We analyze our data with our difference photometry pipeline described in Hu et al. (2024). We perform image subtraction with **Saccadic Fast Fourier Transform (SFFT)** (Hu et al. 2022), a scalable image subtraction algorithm and GPU-enabled implementation of the same that produces difference images up to an order of magnitude faster than widely used tools with comparable accuracy. Aperture photometry is conducted on the resulting difference images using **SExtractor** (Bertin & Arnouts 1996) with fluxes calibrated to the **DESI Legacy Survey (LS)** source catalog and corrected for extinction using the **dustmaps** package (Green 2018) and the

⁴ <https://treasuremap.space/>

$E(B - V)_{\text{SFD}}$ coefficients from [Schlafly & Finkbeiner 2011](#). Our image differencing pipeline detected over 25 million transient features in our campaign data, which we distilled into a tractable list of astrophysical transients through a series of cuts. Table 1 summarizes the vetting steps we applied, which are described in this section.

We first remove any detections on difference images contaminated by bad pixels recorded in the [DECAM CP](#) data quality mask products. Surviving features were then scored using a [Convolutional Neural Network \(CNN\)](#) trained on archival [DECAM](#) data products from our pipeline to perform real/bogus classification. Possible [CNN](#) scores range from 0 to 1, with higher scores associated with more realistic astrophysical objects; at this step we kept any detections with scores greater than 0.7. Roughly 6% of the initial list of detections passed these steps to form our list of real astrophysical detections.

These detections were then cross-matched among themselves to identify features present in data from multiple epochs and filters; the resulting list of transients consisted of 233,313 objects. This list was subsequently crossmatched with the [LS DR10.1](#) catalog ([Dey et al. 2019](#)) and the [Minor Planet Center \(MPC\)](#) service, and any transients respectively matched to star-like sources (defined as a source assigned a [LS](#) morphological type of “PSF”) or minor planets were removed from our search. The [LS](#) crossmatch was also used to sort the sources into three categories based on proximity to the nearest galaxy-type⁵ [LS](#) source: sources within 0.3” of a galaxy-type source were labeled as “A” sources, sources greater than 1.0” away from the nearest such source were labeled as “T” sources, sources falling in the middle ground between these two categories were labeled as “C” sources.

Two final cuts were then applied to limit our search to the most realistic persistent sources, requiring sources to have least two distinct observations separated by >30 minutes, and at least one high-fidelity detection (real/bogus [CNN](#) score ≥ 0.9). Of the remaining 3558 sources, 2388 of them were within 1” of a galaxy-type [LS](#) object (“A” and “C” sources); this final group composed our automated list of candidates based on our photometric [DECAM](#) data. See Table 1 for a summary of cuts applied and resulting numbers of candidates at each cut.

3.2. Additional vetting

Our 2388 automatically-identified sources were then examined by eye to identify candidates for further study. Sources flagged for further investigation included those that had brightened since the time of the [GW](#) event and did not exhibit early reddening (this latter criteria was motivated by the expectation that the luminous counterpart emerges from the depths of the accretion disk, see Figure 1, and we do not expect it to redden as the optical depth decreases). Other considerations included whether there was a perceptible delay time from the [GW](#) event time (reflective of an [EM](#) counterpart needing time to escape the embedding accretion disk before being observed) and whether sources appeared similar to different known transients such as [supernovas \(SNs\)](#). Image stamps were also examined for each source to exclude any artifacts and the like that survived the [CNN](#) cut.

The resulting list was trimmed to remove any transients over 2σ away from the [GW](#) distance posterior, as such information was available. To determine distances to each transient, the [LS](#) galaxy-type object matched to each transient was cross-matched with several galaxy catalogs (with a search radius of 1”) in search of a redshift measurement. Galaxy catalogs used included the [NASA/IPAC Extragalactic Database \(NED\)](#) Local Volume Sample ([Cook et al. 2023](#))⁶, the [Dark Energy Spectroscopic Instrument \(DESI\)](#) galaxy catalog ([DESI Collaboration et al. 2023](#)), and [Quaia](#) ([Storey-Fisher et al. 2024](#)); [LS](#) DR10.1 photometric redshifts were also included. If the host galaxy matched in multiple catalogs, then the best redshift measurement was used, preferring spectroscopic redshifts over [Quaia](#) “spectrophotometric” redshifts ([Storey-Fisher et al. 2024](#)), and the latter over photometric redshifts. Comparing the available redshift measurements to the distance posteriors (taken from the skymap [HEALPix](#)⁷ tile containing the respective transient) informed the elimination of sources beyond the 2σ threshold cut, using the larger of the two uncertainties between the [GW](#) and galaxy catalog measurements. Note that transients whose host galaxy lacked any redshift measurement were not subject to this cut.

Candidates in our shortlist were photometrically classified with [Parameterization of SuperNova Intrinsic Properties \(ParSNIP\)](#) ([Boone 2021](#)), assuming a model trained on the [PLAsTiCC](#) ([Kessler et al. 2019](#)) simulations; because [ParSNIP](#) uses redshift as an input parameter, this classification was limited to only those sources with a redshift measurement. When classifying a light

⁵ We consider all [LS](#) sources with PSF types other than “PSF” (stellar) and “DUP” (extended source components) as “galaxy-type” sources.

⁶ <https://ned.ipac.caltech.edu/>

⁷ <https://healpix.sourceforge.io/>

curve, **ParSNIP** assigns a probability to each of a set list of transient classes so that the total probability sums to 1, with each probability reflecting the relative likeness of the light curve to each class. We note that **ParSNIP** does not contain a catch-all class such as “Other” for use when classifying transients of unfamiliar phenomenology: that is, if a transient is strongly dissimilar to all but one of the classes, it could receive a high classification probability for that one class, even if it not a strong match in and of itself. We consider the “TDE” **ParSNIP** class as the one most similar to the **AGN** flares of interest (all other classes concern some kind of **SN**, except for the **KN** class, whose typical timescales are considerably shorter than those we are interested in). Accordingly, in our use case we broadly interpret transients classified as “TDE” as those that are not identifiable as **SN**-like events, and we refer to the “TDE” class as “Non-**SN**” to better reflect this perspective. We find that most of our classified transients receive this classification.

The final shortlist of 23 transients surviving these cuts is shown in Table 2. We separate several subsets from this list to identify transients that we exclude from our search via asynchronous analysis after our follow-up campaign; these subsets appear in labeled sections of the table. 6 of the transients in our shortlist showed significant brightening, but did not peak during the time they were observed (so potentially consistent with longer-term **AGN** variability), and so we are unable to consider their full nature with our present dataset. 9 transients, while initially interesting for further monitoring, exhibited reddening in later epochs, and so are excluded through disagreement with our assumed counterpart model that predicts a signature that becomes more blue with time. Finally, 2 transients were excluded as counterpart candidates through spectroscopic classification (see §4.2.2 and §4.2.3). The remaining 6 transients are those that cannot be excluded as counterparts to S230922g, and are listed at the top of the table. Table 2 includes host redshift information (where available), along with **GW** skymap localization information: the 1σ distance posterior expressed as redshift under the assumed cosmology, and the 2D and 3D **confidence interval (CI)** as calculated with the `ligo.skymap.postprocess.crossmatch.crossmatch` routine⁸ (Singer et al. 2016). The transients are ranked by ascending 2D **CI**, s.t. the objects in the highest probability regions are listed first. The highest-probability

ParSNIP class and the associated probability are listed in the last two columns of the table, where available.

4. CANDIDATE COUNTERPARTS

In this section we describe candidate counterparts that received particular scrutiny during our campaign, including one we identify as the most likely to be a counterpart to S230922g. While we generally refer to candidates by their **TNS** name, we include the internal name for each of our transients as well, as these names were used for initial reports. Internal names are assembled from the date of discovery and RA/dec of the source; for example, the internal name of C202309242206400m275139 refers to a transient first detected on September 24, 2023 with an RA/dec of 22h 06m 40.0s, -27° 51m 39s (the letter between the RA and dec can be either “p” or “m”, denoting a positive or negative declination, respectively). The leading character in the object names indicates the proximity of the transient to the nearest galaxy-type **LS** source, in the same convention explained in §3.1 (“A” for nuclear sources, “T” for non-nuclear sources, and “C” for marginally nuclear sources). The internal names for all transients in our shortlist can be found in the subfigure titles of Figure 5.

4.1. AT 2023aagj (C202309242206400m275139)

We consider AT 2023aagj to be the transient from our sample most likely to be an optical counterpart to S230922g. This transient is distinguished by a ~ 1 magnitude brightening over a period of a month, remaining blue in color throughout its evolution. It is within 0.5” of the host galaxy centroid, and as such may be associated with activity in the host nucleus. Difference photometry, spectra, and sample stamps for this candidate are visible in Figure 3. **ParSNIP** classifies AT 2023aagj as a “TDE”/“Non-**SN**”-type object with a probability of 94.4%, which in this context distinguishes the transient from **SNs** and the like.

Two spectra of AT 2023aagj were taken before the transient faded. The initial Keck **Low-Resolution Imaging Spectrograph (LRIS)** spectrum, taken on December 7 (PI: Kasliwal, PID: C360), and reduced with the standard LPIPE routine (Perley 2019), revealed ionized gas emission lines and broad line features for the H α and MgII regions, indicating a possible **AGN** host. The redshift of the host was calculated to be 0.184, placing the transient within the 83% credible volume for the S230922g skymap and consistent at the 1.4σ level with the luminosity distance posterior of the **GW** event. An additional spectrum of the object was taken with Gemini

⁸ <https://lscsoft.docs.ligo.org/ligo.skymap/postprocess/crossmatch.html#ligo.skymap.postprocess.crossmatch.crossmatch>

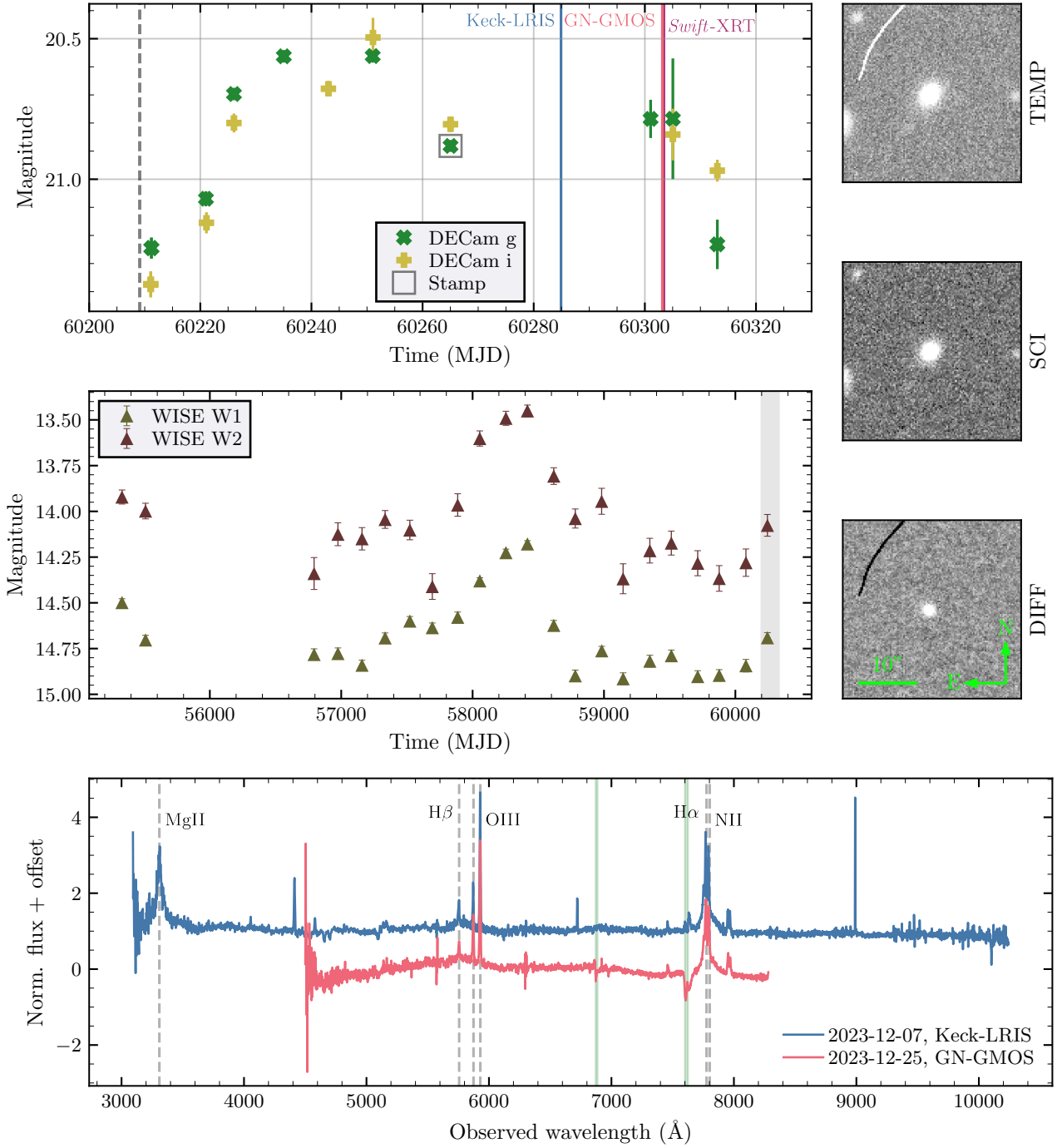


Figure 3. Observational data for AT 2023aagj. *Upper left:* Difference photometry for the transient. $g(i)$ -band data are shown in green (yellow). The colored vertical lines in the light curve plot indicate the times additional data (spectra and X-ray) were taken. *Upper right:* Stamps from the template, science, and difference images for a sample epoch; the epoch from which the sample stamps are taken is outlined in the photometry plot with a gray square. *Center left:* WISE photometry for the host of AT 2023aagj. The span of the difference photometry plot is shaded in gray. *Bottom:* Spectra taken for the transient. Telluric regions are shaded in green. Several known emission lines (shifted according to the measured redshift of the host) are labeled and shown as dashed gray lines.

Table 2. Summary table for our counterpart candidate shortlist. Redshifts are shown as available from crossmatching with several extragalactic databases and direct measurement from our spectra. The luminosity distances and uncertainties are reproduced from the GW skymap, using the `DISTMU` and `DISTSIGMA` values for the HEALPix tile in which the transient is located. The objects are sorted by ascending 2D skymap probability CI, s.t. the objects in the highest probability regions are listed first. The highest probability ParSNIP photometric classification along with the probability are listed in the last two columns; in this work, we rename the ParSNIP class “TDE” as “Non-SN” (see text). The last three subdivisions of the table include transients that did not peak during our observation window, those that reddened in later epochs, and those that were excluded as possible counterparts through spectroscopic classification.

Object	Host redshift		GW skymap			ParSNIP	
	z_{host}	z_{host} source	d_L [Mpc]	2D CI	3D CI	Classification	Prob.
AT 2023adwb	-	-	1360 ± 430	0.136	-	-	-
AT 2023uho	-	-	1250 ± 552	0.484	-	-	-
AT 2023adwp	-	-	1274 ± 433	0.652	-	-	-
AT 2023aagj	0.184	Specz (this work)	1478 ± 425	0.754	0.829	Non-SN	0.944
AT 2023adwt	-	-	1429 ± 413	0.756	-	-	-
AT 2023uea	0.195 ± 0.084	Quaia SPz	1459 ± 426	0.790	0.814	Non-SN	0.991
<i>Transients without peak</i>							
AT 2023adio	0.212 ± 0.097	Quaia SPz	1410 ± 446	0.242	0.363	SNII	0.901
AT 2023adwd	-	-	1328 ± 451	0.285	-	-	-
AT 2023adwe	1.528 ± 0.671	LS photz	1293 ± 463	0.285	-	Non-SN	0.927
AT 2023adwn	0.349 ± 0.078	LS photz	875 ± 486	0.617	0.810	Non-SN	0.676
AT 2023adwq	0.391 ± 0.112	Quaia SPz	1545 ± 454	0.683	0.784	Non-SN	0.968
AT 2023adfo	-	-	1471 ± 422	0.729	-	-	-
<i>Reddening transients</i>							
AT 2023adwc	0.216	NED specz	1228 ± 445	0.143	0.080	Non-SN	0.996
AT 2023adwf	0.180	NED specz	1148 ± 417	0.300	0.155	Non-SN	0.985
AT 2023adwj	-	-	1345 ± 457	0.429	-	-	-
AT 2023uec	-	-	1127 ± 469	0.459	-	-	-
AT 2023uos	-	-	1448 ± 458	0.475	-	-	-
AT 2023adwl	-	-	1051 ± 441	0.583	-	-	-
AT 2023unj	-	-	1127 ± 439	0.642	-	-	-
AT 2023unl	0.248	Specz (this work)	1535 ± 444	0.677	0.652	-	-
AT 2023adws	0.178	NED specz	1451 ± 419	0.750	0.827	Non-SN	0.928
<i>Excluded via spectra</i>							
AT 2023aden	-	-	1154 ± 451	0.658	-	-	-
AT 2023uab	0.128	Specz (this work)	919 ± 479	0.785	0.554	SNIIa	0.814

North Gemini Multi-Object Spectrograph (GMOS) on December 25, 2023 (PI: Cabrera, PID: GN-2023B-DD-109), using a B480 grating with 2x900s dithered exposures and a central wavelength of 6250 Å. The data were reduced with [Data Reduction for Astronomy from Gemini Observatory North and South \(DRAGONS\)](#) ([Labrie et al. 2019](#)), and flexure corrections were applied by re-running the reduction software without sky subtraction, and calculating a scalar offset by comparing to a sky line catalog ([Rousselot et al. 2000](#)). An interesting feature observed in the Keck spectrum is some degree of asymmetry (skewed towards the redder wavelengths) in both the H α and MgII broad lines, as seen in Figure 4; however, the H α asymmetry does not appear in the later Gemini North-GMOS spectrum. The latter spectrum does not cover the MgII feature, and so no comparison between the two times is possible in this regime. Given that there is no similarly-resolved archival spectrum for this source, we are not able to distinguish transient spectral features from persistent host features at this time.

We fit the Gemini spectrum using the Penalized Pixel-Fitting software (ppxf; [Cappellari 2023](#)) in order to study the possible presence of an AGN. We fit the spectrum with stellar templates from the E-MILES SSP library ([Vazdekis et al. 2016](#)) along with a number of narrow and broad Gaussian peaks corresponding to various emission and absorption lines. Using these measured gas line strengths, we place this object in the [Baldwin–Phillips–Terlevich \(BPT\)](#) diagram, finding that it lands in the “composite” region (according to the delineations of [Kewley et al. 2001](#); [Kauffmann et al. 2003](#); [Kewley et al. 2006](#)). This indicates that it is likely that the observed lines are due to a combination of star formation and AGN activity. We further measure the mass of the AGN using the fitted H α velocity dispersion, which we find to be 2282 ± 41 km/s. The resulting BH mass according to the method presented in ([Greene & Ho 2005](#)) is $M_{\text{SMBH}} \sim 2 \times 10^7 M_{\odot}$. Note that this measurement may be inaccurate if the transient is significantly contributing to the BLR emission.

[Wide-field Infrared Survey Explorer \(WISE\)](#) ([Wright et al. 2010a](#)) infrared data for the host of this event is shown in Figure 3. Following [Clark et al. \(2024\)](#), we retrieved this data from the NASA/IPAC infrared science archive (IRSA)⁹, utilizing data from both the ALLWISE ([Wright et al. 2010b](#)) and NEOWISE Reactivation Releases (NEOWISE-R; [Mainzer et al. 2011, 2014](#)). Individual observations are combined following quality control cuts to obtain one mean magnitude per

filter for each observation period, providing a ~ 6 month cadence. Notably, there are variations in the host system of similar amplitude to our detected transient, but it must be recognized that such variations occur on much longer ($\sim 10\times$) timescales than the timescale of AT 2023aagj. We compare this behaviour with publicly available PanSTARRS ([Flewelling et al. 2020](#)) and DECam images at this location, which, although sparse, do not show any significant change in flux. We observe that a significant jump of ~ 0.3 mag in g band 5” aperture magnitude occurred according to the SkyMapper data release ([Onken et al. 2024](#)) between MJD ~ 57650 and ~ 57850 . It is possible that an associated optical signature existed in that time period, but was missed by the relatively sparse nature of the optical observations, and the infrared (IR) component we observed was delayed from the optical via dust reprocessing. We do not observe a rebrightening of the source in the WISE bands over the timescale of the optical transient, but there appears to be a ~ 0.1 increase in magnitude in December 2023, potentially indicating the start of a reprocessed, delayed emission from the event.

We also produce a [WISE](#) color-color plot for W1-W2 versus W2-W3, although this is not shown as W3 is only available in one epoch, which may not be representative of the entire color evolution of the object over the past years. By comparison with populations of extragalactic objects (as defined in [Wright et al. 2010a](#)) we find that while the host most clearly lies in the [WISE](#) population regions associated with spiral and luminous infrared galaxies, it is near the boundary into the Seyfert and quasar parameter spaces, and has been observed to temporarily visit these regions.

We carried out a [ToO](#) observation of AT 2023aagj with the *Neil Gehrels Swift Observatory* ([Gehrels et al. 2004](#)) X-ray Telescope (XRT; [Burrows et al. 2005](#)). Our observation began on 2023-12-25 at 06:02 UT with a total exposure of 3265 s in [Photon Counting \(PC\)](#) mode. We used the *Swift*-XRT automated tools ([Evans et al. 2009, 2023](#)) to analyze our data and all previous data covering the source position from May 2006 and April 2021 (totaling 7.8 ks exposure in PC mode, including the latest data). We measure a source position of RA, DEC (J2000) = $22^{\text{h}}06^{\text{m}}40^{\text{s}}.26$, $-27^{\circ}51'41.8''$ with an uncertainty radius of $4.7''$ (90% confidence). In our latest observation the source displays a soft spectrum with all photon counts below 5 keV, similar to the previous observations. The time-averaged spectra were fit with an absorbed powerlaw model using XSPEC v12.14.0 ([Arnaud 1996](#)) within HEASoft v6.32. The inferred photon index is relatively unconstrained but favors $\Gamma \approx 2.5$ with hydrogen column density $N_H \approx 2 \times 10^{20} \text{ cm}^{-2}$. The un-

⁹ <https://irsa.ipac.caltech.edu/>

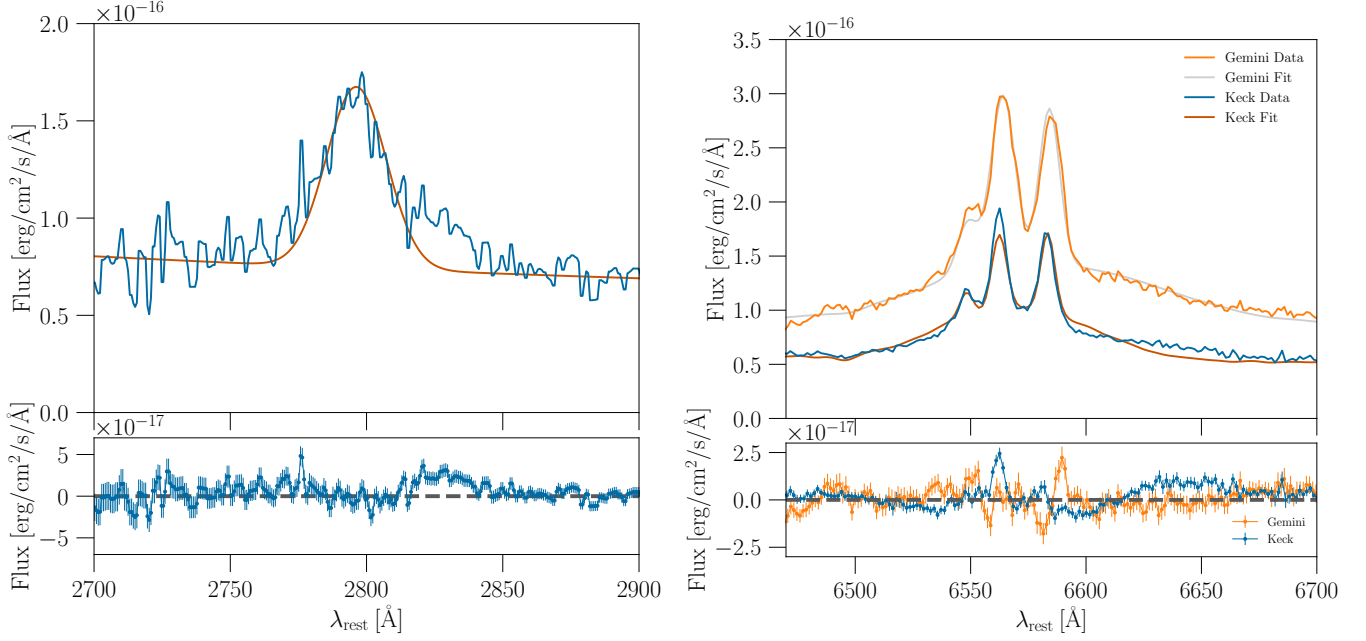


Figure 4. pPXF model and data for the two AT 2023aagj spectra around the two broad lines of interest. The bottom panels show the residuals between the model and data. An asymmetry redward of the line appears to be present in the Keck spectrum, taken closer to peak, but disappears in the later Gemini spectrum.

absorbed flux (0.3 – 10 keV) is $F_X = (3.2^{+8.8}_{-1.0}) \times 10^{-13}$ erg cm $^{-2}$ s $^{-1}$ in our latest observation. We find a factor of ~ 4 increase in flux between the 2006 and 2021 observations, but no significant change (a factor of $\sim 1.2 \pm 0.5$) between 2021 and 2023 (due also to the larger errors on the flux). We therefore conclude that there is no ongoing X-ray outburst from AT 2023aagj, although we note that these observations were taken ~ 2 months after the optical peak at a time when any additional flux from the transient may have been too faint to be detected. It is interesting to note how the *WISE* flare peaked around 2018, notably coincident with the significant change in X-ray flux. We speculate this may be related to a changing look AGN event, although this is hard to confirm due to the lack of an older spectrum.

4.2. Other candidates of scrutiny

We took spectra for three additional candidates beyond AT 2023aagj during our follow-up campaign. The spectrum for one transient (AT 2023unl) provides inconclusive evidence for the nature of the source; however, the source was observed to redden in later epochs, and so is disfavored by our assumed counterpart model. The spectra for the other two transients (AT 2023aden and AT 2023uab) contain SN-like features; both of these transients are subsequently excluded as possible counterparts to S230922g. The three spectra are shown in Figure 9 (Appendix A).

4.2.1. AT 2023unl (C202310042207549m253435)

The spectrum for AT 2023unl was taken by the Robert Stobie Spectrograph (RSS) (Burgh et al. 2003; Kobulnicky et al. 2003) on the South African Large Telescope (SALT) (Buckley et al. 2006). The RSSMOSPipeline (Hilton et al. 2018)¹⁰ was used for the reduction of SALT-RSS data. The pipeline automatically identifies and extracts one dimensional spectra using the data products delivered by the SALT observation team. Using the known redshift of the observed object and the reduced spectra, PYQSOFit (Guo et al. 2018)¹¹ was then used to fit and identify possible emission lines in the data. The signal-to-noise ratio (SNR) for the spectrum is relatively low, with few strong features. The present H β line does not demonstrate any unusual characteristics such as asymmetry. A possible broad line feature is present around an observed wavelength of 5525 Å, albeit a chip gap appears to have ended up at the peak of the feature, and so it is uncertain how much of the observed variation is due to imperfect data reduction; that said, there is no similar feature around the second chip gap near 6575 Å. We conclude there is no conclusive evidence for this transient being in an AGN.

¹⁰ <https://github.com/mattyowl/RSSMOSPipeline>

¹¹ <https://github.com/legolason/PyQSOFit>

4.2.2. AT 2023aden (A202310262246341m291842)

A spectrum was taken for this transient using Gemini North **GMOS** on November 16, 2023 (PI: Cabrera, PID: GN-2023B-DD-103), and was acquired and reduced in a similar manner as the Gemini spectrum for AT 2023aagj, with a central wavelength of 7600 Å. The spectrum is blue and has strong absorption features characteristic of **SNs**; subsequently, we do not consider this transient as a likely counterpart to S230922g.

4.2.3. AT 2023uab (C202309242248405m134956)

We used the Double Spectrograph (DBSP) mounted at the 200-inch Hale Telescope at Palomar Observatory. For this source, we used a 1.5 arcsec slitmasks, a D55 dichroic, a blue grating of 600/4000 and red grating of 316/7500. The data were reduced using a custom PyRAF DBSP reduction pipeline (Bellm & Sesar 2016). The spectrum exhibits clear H α and H β features which enable a redshift measurement of 0.128 (computed with Redrock¹²; Bailey et al., in prep.). The continuum of the spectrum peaks around ~ 5000 Å, with several broad absorption features present around the peak. This, in concert with ParSNIP classifying the object as a type Ia **SN**, leads us to exclude this object as a possible counterpart.

5. DISCUSSION

Taking our favored counterpart candidate of AT 2023aagj, we work under the assumption that the transient is related to S230922g and try to infer whether the the properties of the flare may be consistent with expectations for the counterpart signal, mechanism, and host.

What can be noted is that the persistent blue color is unlike typical supernovae, and **structure function** (SF) arguments as in Palmese et al. (2021) show that this transient is distinguished from typical **AGN** activity at the 5.9σ level (corresponding to a one-sided probability $p_{\text{flare}} \sim \mathcal{O}(10^{-16})$). Taking the 90% **CI** volume of the event as $3.73 \times 10^8 \text{ Mpc}^3$ (as calculated with **ligo.skymap**) and a fiducial **AGN** number density of $10^{-4.75} \text{ Mpc}^{-3}$ (Bartos et al. 2017a; Greene & Ho 2007), we estimate a count of 6600 **AGN** in the volume. Alternatively, crossmatching the Milliquas (Flesch 2023) quasar catalog with the skymap (also with **ligo.skymap**) yields a 3D match of 826 objects. Given the discovery window of our follow-up campaign $t_{\text{window}} = 92$ days (calculated as the difference in time between the second epoch and the last), we calculate the

probability of a chance discovery of a similar flare as

$$p_{cc} = n_{\text{AGN}} \frac{t_{\text{window}}}{\Delta t_{\text{rise}}} p_{\text{flare}} \approx \left(4.48 \times 10^{-16} \frac{\text{flares}}{\text{AGN}} \right) n_{\text{AGN}}, \quad (1)$$

which predicts $p_{cc} \sim \mathcal{O}(10^{-12})$ and $p_{cc} \sim \mathcal{O}(10^{-13})$ for the number density and Milliquas estimates, respectively.

We compare our candidate flare with the sample of **Zwicky Transient Facility** (ZTF) transients from Graham et al. (2023). Assuming a roughly constant spectral flux density across the g - and B -band frequency domain, we apply the B bandpass bolometric correction of 5.15 from Duras et al. (2020) to derive a total flare energy of

$$E_{\text{tot}} \approx 4\pi d_L^2 \left(5.15 \int d\nu T_B(\nu) \right) \int_{t_d}^{t_e} dt 10^{-0.1m_{g,\text{AB}}(t)+48.6} \\ \approx 1.2 \times 10^{50} \text{ erg}, \quad (2)$$

where $T_B(\nu)$ is the transmission function for the B bandpass (Bessell 1990), and t_d and t_e are the times of the first and last observations of the flare. Fitting a Gaussian rise-exponential decay model to the g -band light curve yields a rise time parameter (the standard deviation of the Gaussian) of $t_{\text{rise}} \approx 5.25$ days. This places this transient in an intermediate regime between the **SN** and **TDE** populations from Graham et al. 2023 (c.f. Figure 2 in that paper) among fast **TDEs** and high-energy **SNs**. Notably, the Graham et al. 2023 proposed flare counterparts are all slower and more energetic than AT 2023aagj; this may be associated with the measurement of our flare parameters being based on difference photometry, while the ZTF light curves used in the compared study are assembled via direct photometry that includes the flux of the host **AGN**.

We estimate physical parameters of the system following the methodology of Graham et al. (2020), which tests the hypothesis that the flare is generated from a Bondi accreting **BH** as the remnant emerges from the accretion disk due to a post-merger kick. With a flare onset time delay of ~ 2 days from the **GW** trigger and total mass estimate of $M_{\text{tot}} \sim 90M_{\odot}$, under the assumption of association we can conclude one or more of the following: either (i) the kick velocity v_{kick} is large, or (ii) the disk is geometrically thin (aspect ratio $h \leq \mathcal{O}(10^{-3})$) or (iii) the disk is not optically thick away from a geometrically thin mid-plane, or (iv) there is a cavity in the disk due to feedback from the pre-merger **BBH**.

We continue by assuming the kick velocity is not specially large or small. If we assume a kick velocity $v_{\text{kick}} \sim \mathcal{O}(200)\text{km/s}$ (which is consistent with the peak of the prior in Varma et al. 2022) then we can constrain

¹² <https://github.com/desihub/redrock>

the approximate disk height from (Graham et al. 2023)

$$t_{\text{exit}} \sim \frac{H \sqrt{2 \ln \tau_{\text{mp}}}}{v_{\text{kick}}} \quad (3)$$

where H is the disk height and τ_{mp} is the mid-plane optical depth. Since $t_{\text{exit}} \sim 2$ days, $\tau_{\text{mp}} \sim 10^{[3,6]}$ yields a factor 4 – 5 from the square root, so $H \sim 0.3 r_g (M_{\text{SMBH}}/2 \times 10^7 M_\odot)$. This implies a thin disk, possibly similar to the thin regions of a Thompson et al. (2005) model, which also has a lower τ_{mp} than other models such as Sirko & Goodman (2003). The thinner regions of AGN disks are where gas damping is most efficient and consequently where mergers are more likely to occur (McKernan & Ford 2024).

If we assume from Figure 3 that the flare begins 2 days post-S230922g (denoted by a vertical line), and the flare lasts through the spectra denoted by the blue and red lines, then the overall flare duration is $t_{\text{flare}} \sim \mathcal{O}(10^2)$ days. Given $E_{\text{tot}} \sim 10^{50}$ erg, the average luminosity of the flare is $\bar{L}_{\text{flare}} \sim 10^{43}$ erg/s, which can be parameterized as $\bar{L}_{\text{flare}} \sim 10^3 L_{\text{Edd}} (M_{\text{BBH}}/90 M_\odot)$ where L_{Edd} is the Eddington luminosity. If we parameterize the Bondi accretion rate onto the merged BH (\dot{M}_{BHL}) as:

$$\dot{M}_{\text{BHL}} \sim \frac{0.03 M_\odot}{\text{yr}} \left(\frac{M_{\text{BBH}}}{90 M_\odot} \right)^2 \times \left(\frac{v_{\text{rel}}}{200 \text{ km/s}} \right)^{-3} \left(\frac{\rho_{\text{disk}}}{10^{-11} \text{ g/cm}^3} \right) \quad (4)$$

where ρ_{disk} is the disk gas density and we assume the relative velocity (v_{rel}) between the BH and the AGN disk gas is $v_{\text{rel}} \sim v_{\text{kick}}$, i.e. the sound speed in the AGN disk gas is less than v_{kick} . We have chosen ρ_{disk} to be comparable to the typical density in a Thompson et al. (2005) model where the disk is near its thinnest (aspect ratio $h \sim 10^{-3}$). Then $L_{\text{flare}} \sim 10^{-2} L_{\text{BHL}}$, where $L_{\text{BHL}} = \eta \dot{M}_{\text{BHL}} c^2$. Interestingly, this accretion rate is within an order of magnitude of the inferred accretion rate onto embedded BBH in AGN from recent GRMHD simulations (Dittmann et al. 2024).

Associating the line asymmetry with an off-center flare implies that the signature persists in the BLR for ~ 70 days post event, but is gone ~ 90 days post event. A light-travel time across the full BLR of $\mathcal{O}(90)$ days (~ 80 in rest frame), corresponds to a distance scale of $0.07 \text{ pc} \sim 7 \times 10^4 r_g (M_{\text{SMBH}}/2 \times 10^7 M_\odot)$, implying that the merger occurred around $4 \times 10^4 r_g (M_{\text{SMBH}}/2 \times 10^7 M_\odot)$. This is located further out than the thinnest regions of a Sirko & Goodman (2003) model disk, so we can rule out an origin in a disk similar to that model. This location could be consistent with the thinnest ($h \sim$

10^{-3}) regions of a Thompson et al. (2005) model disk, which extend $\mathcal{O}[0.01, 0.1] \text{ pc}$.

An alternative candidate for an off-center luminous flare in an AGN is a μ -TDE, where a star is tidally disrupted by a stellar mass BH embedded in an AGN disk. Perna et al. (2021) show that in the outer regions ($\sim 7 \times 10^4 r_g (M_{\text{SMBH}}/2 \times 10^7 M_\odot)$) of a Thompson et al. (2005) disk model, a μ -TDE will peak in afterglow very quickly (\sim hours), which is inconsistent with our observations. However, if M_{SMBH} is actually a factor of a few more massive, then the diffusion time becomes longer, potentially months, which could be consistent with our observations.

We also note that the lightcurve of AT 2023aagj resembles those of afterglows in AGN disks as found in Wang et al. (2022). The rise of an afterglow from a BBH merger is not implausible, assuming that these objects are able to launch jets, as explored by Tagawa et al. (2023). Future work could investigate the possibility of fitting those afterglow models in high-density environments.

Under the assumption that AT 2023aagj is the counterpart to S230922g, our requirements are that the AGN disk must be relatively thin, similar to a Thompson et al. (2005) model, and that the accretion rate onto the kicked BH is significantly super-Eddington, but well below the Bondi rate (and requires an associated jet for the radiation to emerge). One of our most likely false positive for this event is a μ -TDE in the disk if our estimate of M_{SMBH} is too small by a factor of a few.

6. CONCLUSIONS

In this work we present the results of the GW-MMADS follow-up of S230922g. We discuss in detail our most likely candidate AT 2023aagj, noting it is mostly constant blue color, AGN-hosted nature, and especially the presence of asymmetry in BLR spectral features as evidence in favor of recognizing it as a counterpart to S230922g. However, we do not find the current dataset sufficient to clearly identify the transient as such.

It is worth noting that several aspects lead to an inconclusive outcome regarding the significance of this association. The variable nature of the AGN in question, showing a significant flare in the infrared and a change in X-ray flux over the past decade, exemplifies that there is some inherent activity in the host, and the discovery of a GW counterpart is only possible if a means of distinguishing the transient signal from any host variability. One possible discriminator is the observation of asymmetric components in the broad lines of the AGN spectrum, indicative of an off-center phenomenon; however, other sources such as disk winds and tilted dust ob-

scuration may cause similar profiles. A smoking gun for the BBH association would be the evolution of the asymmetric component in sync with the transient light curve, with the asymmetry shifting towards bluer wavelengths and eventually disappearing as the transient fades. For AT 2023aagj, due to the lack of wavelength coverage for the Gemini spectrum and subsequent lack of multiple observations of MgII, a chip gap on H β in the Keck spectrum, the telluric region blueward of H α , and the target setting in December, the extraction of such an evolution is not feasible with the present data. A spectrum of this object in 2024 as the target rises again may be informative about the nature of the asymmetry. A persistent line asymmetry long after the merger event may point to similarly persistent asymmetric illumination in this source, such as a warped disk, and could rule out the association between AT 2023aagj and S230922g. Finally, given the blue color and the ParSNIP prediction, we cannot exclude that this transient may have originated from a TDE.

We consider the uncertainty of our result as another indicator of the challenging nature of the search for BBH EM counterparts and successively the need for the continuation and growth of future efforts for this purpose. More so than for NS merger counterparts, predictions of BBH counterparts share a parameter space with existing transient families (e.g. that of TDEs) and AGN variability, and distinguishing between the different classes of events at the present time may be challenging. Spectroscopic data are expected to be the most helpful towards this end, and so it is important to combine the appropriate resources with photometric follow-up while transients are still active, for as long as it takes to develop models mature enough to perform well without requiring such expensive resources. This is especially relevant for the remainder of O4 follow-up, as all efforts made now will be the last for GW follow-up until the fifth gravitational wave observing run (O5) begins in 2027. With Virgo having joined the GW detector network for O4b, we expect future O4 searches to yield better localized events, a trend that is expected to continue with O5; these lower search volumes, in concert with forthcoming powerful resources such as Legacy Survey of Space and Time (LSST) (Ivezic et al. 2019), will help future counterpart searches be more efficient and effective, and will help deepen and broaden the impact of GW and multimessenger astronomy in the years to come.

ACKNOWLEDGEMENTS

TC, AP, and LH acknowledge that this material is based upon work supported by NSF Grant No. 2308193. BO gratefully acknowledges support from the

McWilliams Postdoctoral Fellowship at Carnegie Mellon University. BM & KESF are supported by NSF AST-2206096 and NSF AST-1831415 and Simons Foundation Grant 533845 as well as Simons Foundation sabbatical support. The Flatiron Institute is supported by the Simons Foundation. AP thanks Rosalba Perna, Armin Rest, and Stephen Smartt for useful discussion.

This research used resources of the National Energy Research Scientific Computing Center, a DOE Office of Science User Facility supported by the Office of Science of the U.S. Department of Energy under Contract No. DE-AC02-05CH11231 using NERSC award HEP-ERCAP0029208 and HEP-ERCAP0022871. This work used resources on the Vera Cluster at the Pittsburgh Supercomputing Center (PSC). We thank T.J. Olesky and the PSC staff for help with setting up our software on the Vera Cluster. MWC acknowledges support from the National Science Foundation with grant numbers PHY-2308862 and PHY-2117997.

This project used data obtained with the Dark Energy Camera (DECam), which was constructed by the Dark Energy Survey (DES) collaboration. Funding for the DES Projects has been provided by the US Department of Energy, the US National Science Foundation, the Ministry of Science and Education of Spain, the Science and Technology Facilities Council of the United Kingdom, the Higher Education Funding Council for England, the National Center for Supercomputing Applications at the University of Illinois at Urbana-Champaign, the Kavli Institute for Cosmological Physics at the University of Chicago, Center for Cosmology and Astrophysics at the Ohio State University, the Mitchell Institute for Fundamental Physics and Astronomy at Texas A&M University, Financiadora de Estudos e Projetos, Fundação Carlos Chagas Filho de Amparo à Pesquisa do Estado do Rio de Janeiro, Conselho Nacional de Desenvolvimento Científico e Tecnológico and the Ministério da Ciência, Tecnologia e Inovação, the Deutsche Forschungsgemeinschaft and the Collaborating Institutions in the Dark Energy Survey.

The Collaborating Institutions are Argonne National Laboratory, the University of California at Santa Cruz, the University of Cambridge, Centro de Investigaciones Energéticas, Medioambientales y Tecnológicas–Madrid, the University of Chicago, University College London, the DES-Brazil Consortium, the University of Edinburgh, the Eidgenössische Technische Hochschule (ETH) Zürich, Fermi National Accelerator Laboratory, the University of Illinois at Urbana-Champaign, the Institut de Ciències de l’Espai (IEEC/CSIC), the Institut de Física d’Altes Energies, Lawrence Berkeley National Laboratory, the Ludwig-Maximilians Universität at

Munich and the associated Excellence Cluster Universe, the University of Michigan, NSF’s NOIRLab, the University of Nottingham, the Ohio State University, the OzDES Membership Consortium, the University of Pennsylvania, the University of Portsmouth, SLAC National Accelerator Laboratory, Stanford University, the University of Sussex, and Texas A&M University.

Based on observations at Cerro Tololo Inter-American Observatory, NSF’s NOIRLab (NOIRLab Prop. ID 2022B-715089; PI: Palmese; 2023B-851374, PI: Andreoni & Palmese; 2023B-735801, PI: Palmese & Wang), which is managed by the Association of Universities for Research in Astronomy (AURA) under a cooperative agreement with the National Science Foundation. We thank Kathy Vivas, Alfredo Zenteno, and CTIO staff for their support with DECam observations.

Based on observations obtained at the international Gemini Observatory (Prop. ID GN-2023B-DD-103, PI: Cabrera; GN-2023B-109, PI: Cabrera), a program of NSF NOIRLab, which is managed by the Association of Universities for Research in Astronomy (AURA) under a cooperative agreement with the U.S. National Science Foundation on behalf of the Gemini Observatory partnership: the U.S. National Science Foundation (United States), National Research Council (Canada), Agencia Nacional de Investigación y Desarrollo (Chile), Ministerio de Ciencia, Tecnología e Innovación (Argentina), Ministério da Ciência, Tecnologia, Inovações e Comunicações (Brazil), and Korea Astronomy and Space Science Institute (Republic of Korea). Gemini data were processed using DRAGONS (Data Reduction for Astronomy from Gemini Observatory North and South).

This work was enabled by observations made from the Gemini North telescope, located within the Maunakea Science Reserve and adjacent to the summit of Maunakea. We are grateful for the privilege of observing the Universe from a place that is unique in both its astronomical quality and its cultural significance.

Some of the observations reported in this paper were obtained with the Southern African Large Telescope (SALT).

The Legacy Surveys consist of three individual and complementary projects: the Dark Energy Camera Legacy Survey (DECaLS; Proposal ID 2014B-0404; PIs: David Schlegel and Arjun Dey), the Beijing-Arizona Sky Survey (BASS; NOAO Prop. ID 2015A-0801; PIs: Zhou Xu and Xiaohui Fan), and the Mayall z-band Legacy Survey (MzLS; Prop. ID 2016A-0453; PI: Arjun Dey). DECaLS, BASS and MzLS together include data obtained, respectively, at the Blanco telescope, Cerro Tololo Inter-American Observatory, NSF’s NOIRLab; the Bok telescope, Steward Observatory, University of

Arizona; and the Mayall telescope, Kitt Peak National Observatory, NOIRLab. Pipeline processing and analyses of the data were supported by NOIRLab and the Lawrence Berkeley National Laboratory (LBNL). The Legacy Surveys project is honored to be permitted to conduct astronomical research on Iolkam Du’ag (Kitt Peak), a mountain with particular significance to the Tohono O’odham Nation. LBNL is managed by the Regents of the University of California under contract to the U.S. Department of Energy.

BASS is a key project of the Telescope Access Program (TAP), which has been funded by the National Astronomical Observatories of China, the Chinese Academy of Sciences (the Strategic Priority Research Program “The Emergence of Cosmological Structures” Grant XDB09000000), and the Special Fund for Astronomy from the Ministry of Finance. The BASS is also supported by the External Cooperation Program of Chinese Academy of Sciences (Grant 114A11KYSB20160057), and Chinese National Natural Science Foundation (Grant 12120101003, 11433005).

The Legacy Survey team makes use of data products from the Near-Earth Object Wide-field Infrared Survey Explorer (NEOWISE), which is a project of the Jet Propulsion Laboratory/California Institute of Technology. NEOWISE is funded by the National Aeronautics and Space Administration.

The Legacy Surveys imaging of the DESI footprint is supported by the Director, Office of Science, Office of High Energy Physics of the U.S. Department of Energy under Contract No. DE-AC02-05CH1123, by the National Energy Research Scientific Computing Center, a DOE Office of Science User Facility under the same contract; and by the U.S. National Science Foundation, Division of Astronomical Sciences under Contract No. AST-0950945 to NOAO.

This research has made use of the NASA/IPAC Extragalactic Database (NED), which is funded by the National Aeronautics and Space Administration and operated by the California Institute of Technology.

Facilities: Blanco (DECam), Keck:I (LRIS), Gemini:South (GMOS), SALT (RSS), Hale (DBSP), WO:2m (3KK)

Software: astropy (Astropy Collaboration et al. 2013, 2018, 2022), DRAGONS (Labrie et al. 2019), dustmaps (Green 2018), gwemopt (Coughlin et al. 2018), healpy (Górski et al. 2005; Zonca et al. 2019), ppxf (Cappellari 2023), Fritz SkyPortal (Coughlin et al. 2023), ligo.skymap (Singer et al. 2016), LPIPE (Perley 2019), matplotlib (Hunter 2007), numpy (Harris et al. 2020), pandas (McKinney 2010), ParSNIP (Boone 2021), pyraf

dbsp (Bellm & Sesar 2016), Redrock (<https://github.com/desihub/redrock>), SExtractor (Bertin & Arnouts 1996), SFFT (Hu et al. 2022), SWarp (Bertin et al. 2002)

APPENDIX

A. ADDITIONAL DATA

This section contains light curves (Figures 5-8) and spectra (Figure 9) for all candidates other than AT 2023aagj.

For some transients we took additional data with the **Three Channel Camera (3KK)** (Lang-Bardl et al. 2016) at the 2.1m-Fraunhofer Wendelstein Telescope (Hopp et al. 2014) located in the German alps. The instrument is capable of taking three images at the same time in two optical passbands and one **near-infrareds (NIRs)** band. For the monitoring of the transients we used the g , i and J bands. The data were reduced with a pipeline developed at the University Observatory Munich. For the detrending of the images the pipeline makes use of the tools from Gössl & Riffeser (2002). Then the images are calibrated and coadded using **SExtractor** (Bertin & Arnouts 1996), **SCAMP** (Bertin 2006) and **SWarp** (Bertin et al. 2002), difference photometry is conducted with **SFFT** (Hu et al. 2022), and extinction corrections are applied as described in §3.1. During this process, the astrometric solution is computed against the *Gaia* EDR3 catalog (Gaia Collaboration et al. 2016, 2021) and the zero points for the optical bands are calibrated with the **PanSTARRS 1s (PS1s)** catalog (Magnier et al. 2013). The **NIRs** zero points are matched to the **Two Micron All Sky Surveys (2MASSs)** catalog (Skrutskie et al. 2006) and converted to AB magnitudes (Blanton & Roweis 2007). Wendelstein data are plotted as outlined diamonds in Figure 5, with g , i , and J band data plotted in green, yellow, and red, respectively.

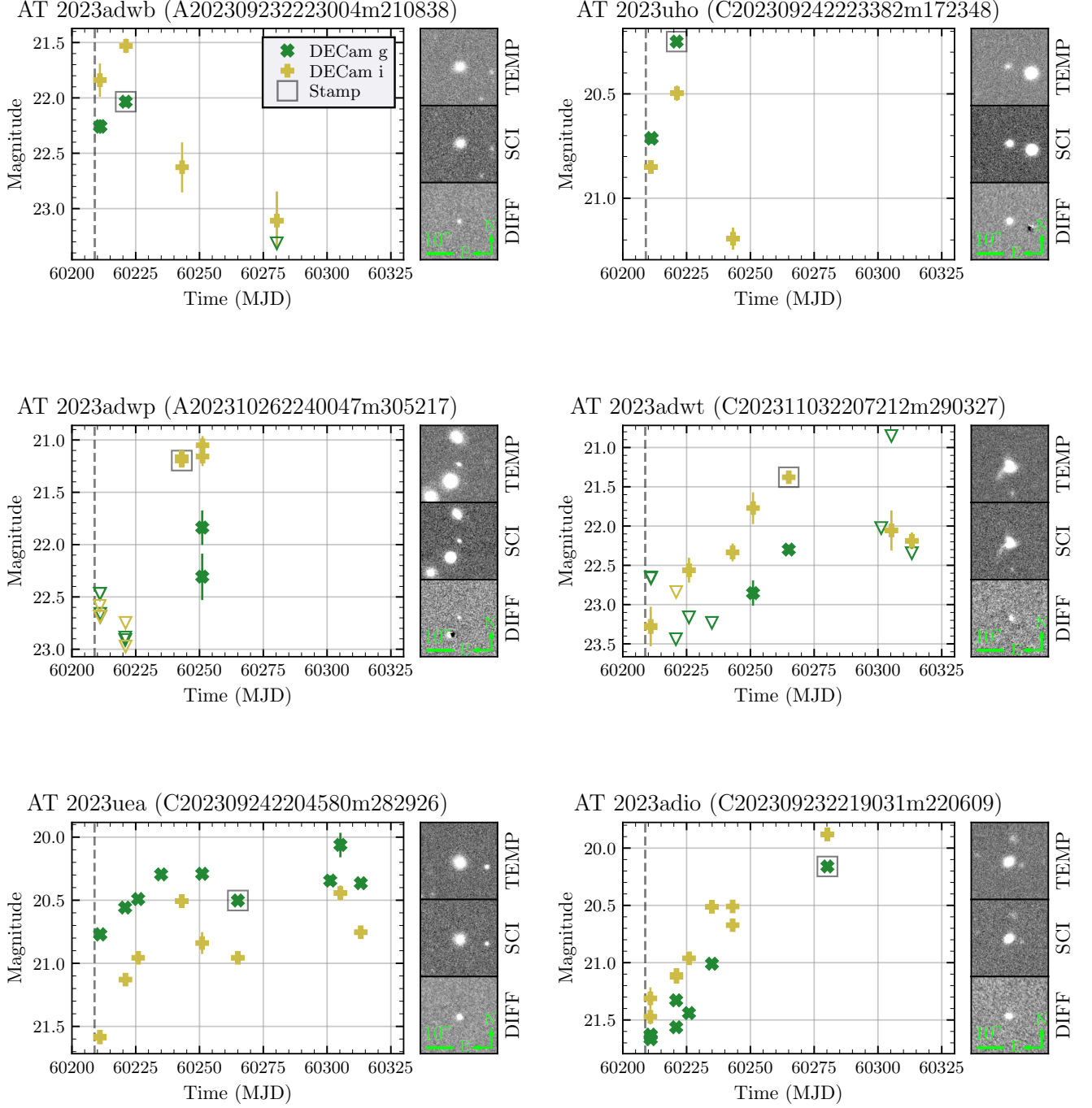


Figure 5. Light curves for our remaining 22 candidates (continued in following figures). The dashed line indicates the S230922g event time. The sample stamps for each transient are taken from the exposure with the highest SNR, indicated with a gray square. Data taken with Wendelstein appear as small diamonds, where relevant (the red point for AT 2023uab is J -band).

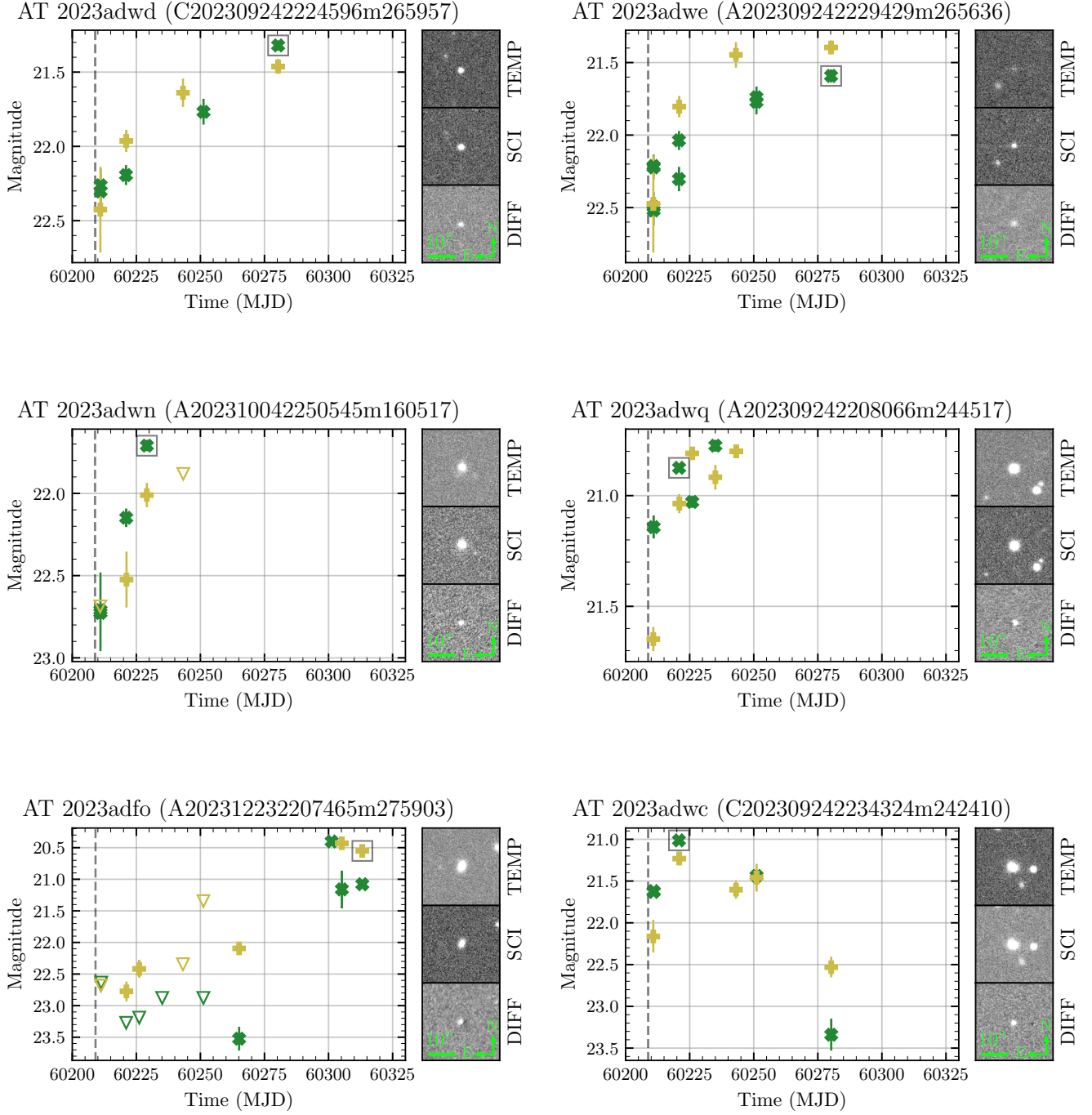
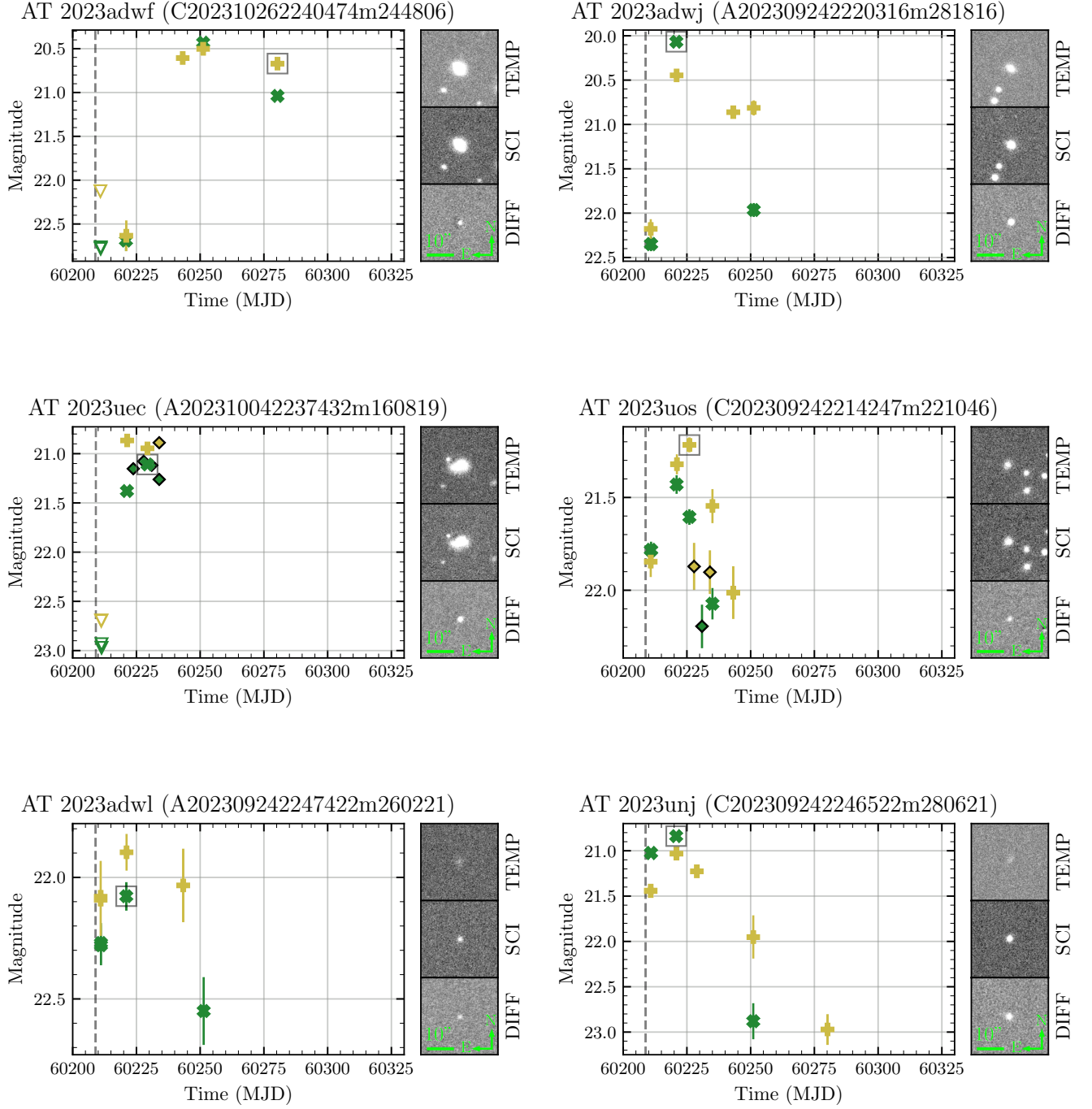


Figure 6. Light curves for our remaining 22 candidates (cont.).

**Figure 7.** Light curves for our remaining 22 candidates (cont.).

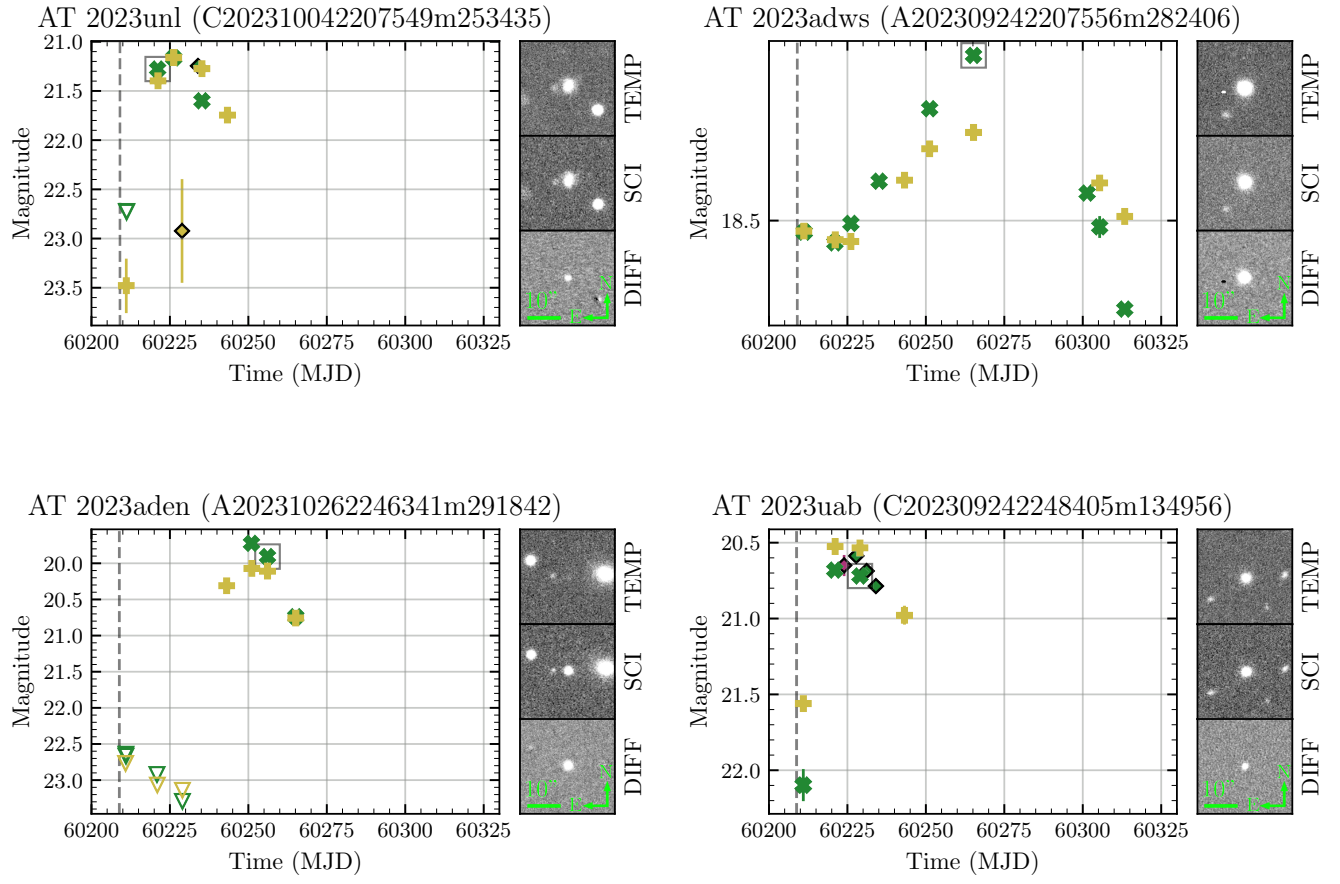


Figure 8. Light curves for our remaining 22 candidates (cont.).

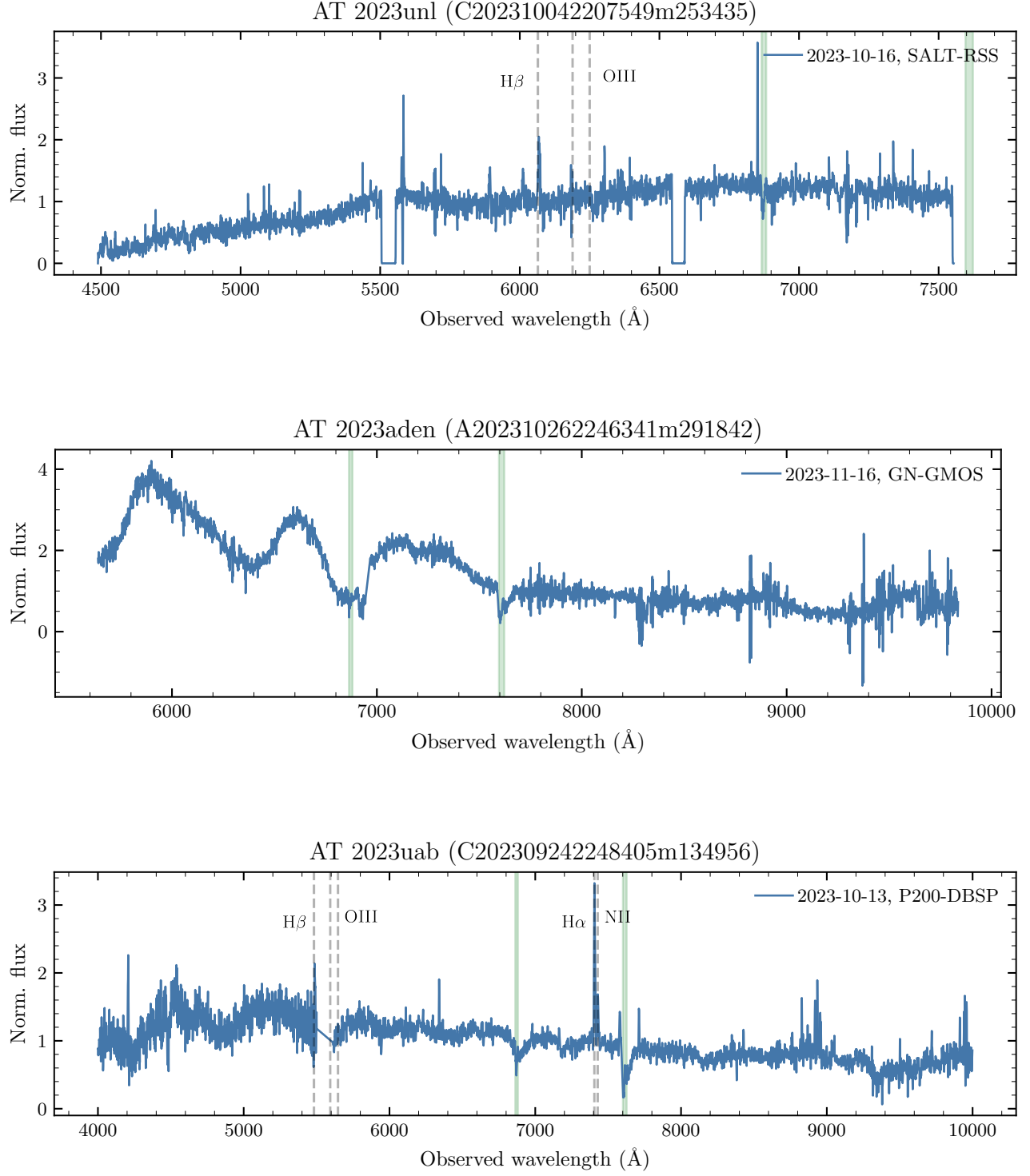


Figure 9. Additional spectra taken as a part of our follow-up campaign. A selection of spectral lines and telluric features are marked as in Figure 3.

REFERENCES

- Abbott, B. P., Abbott, R., Abbott, T. D., et al. 2017a, *The Astrophysical Journal*, 848, L12, doi: [10.3847/2041-8213/aa91c9](https://doi.org/10.3847/2041-8213/aa91c9)
- . 2017b, *The Astrophysical Journal*, 848, L13, doi: [10.3847/2041-8213/aa920c](https://doi.org/10.3847/2041-8213/aa920c)
- . 2017c, *Nature*, 551, 85, doi: [10.1038/nature24471](https://doi.org/10.1038/nature24471)
- . 2018, *Physical Review Letters*, 121, 161101, doi: [10.1103/PhysRevLett.121.161101](https://doi.org/10.1103/PhysRevLett.121.161101)
- Alves, L. M. B., Sullivan, A. G., Yang, Y., et al. 2024, *Monthly Notices of the Royal Astronomical Society*, 531, 3679–3683, doi: [10.1093/mnras/stae1360](https://doi.org/10.1093/mnras/stae1360)
- Andreoni, I., Ackley, K., Cooke, J., et al. 2017, *PASA*, 34, e069, doi: [10.1017/pasa.2017.65](https://doi.org/10.1017/pasa.2017.65)
- Andreoni, I., Goldstein, D. A., Anand, S., et al. 2019, *The Astrophysical Journal*, 881, L16, doi: [10.3847/2041-8213/ab3399](https://doi.org/10.3847/2041-8213/ab3399)
- Andreoni, I., Goldstein, D. A., Kasliwal, M. M., et al. 2020, *The Astrophysical Journal*, 890, 131, doi: [10.3847/1538-4357/ab6a1b](https://doi.org/10.3847/1538-4357/ab6a1b)
- Annis, J., Soares-Santos, M., Berger, E., et al. 2016, *The Astrophysical Journal Letters*, 823, L34, doi: [10.3847/2041-8205/823/2/L34](https://doi.org/10.3847/2041-8205/823/2/L34)
- Arcavi, I., Hosseinzadeh, G., Howell, D. A., et al. 2017, *Nature*, 551, 64, doi: [10.1038/nature24291](https://doi.org/10.1038/nature24291)
- Arnaud, K. A. 1996, in *Astronomical Society of the Pacific Conference Series*, Vol. 101, *Astronomical Data Analysis Software and Systems V*, ed. G. H. Jacoby & J. Barnes, 17
- Ashton, G., Hübner, M., Lasky, P. D., et al. 2019, *The Astrophysical Journal Supplement Series*, 241, 27, doi: [10.3847/1538-4365/ab06fc](https://doi.org/10.3847/1538-4365/ab06fc)
- Astropy Collaboration, Robitaille, T. P., Tollerud, E. J., et al. 2013, *Astronomy and Astrophysics*, 558, A33, doi: [10.1051/0004-6361/201322068](https://doi.org/10.1051/0004-6361/201322068)
- Astropy Collaboration, Price-Whelan, A. M., Sipőcz, B. M., et al. 2018, *The Astronomical Journal*, 156, 123, doi: [10.3847/1538-3881/aabc4f](https://doi.org/10.3847/1538-3881/aabc4f)
- Astropy Collaboration, Price-Whelan, A. M., Lim, P. L., et al. 2022, *The Astrophysical Journal*, 935, 167, doi: [10.3847/1538-4357/ac7c74](https://doi.org/10.3847/1538-4357/ac7c74)
- Bartos, I., Haiman, Z., Marka, Z., et al. 2017a, *Nature Communications*, 8, 831, doi: [10.1038/s41467-017-00851-7](https://doi.org/10.1038/s41467-017-00851-7)
- Bartos, I., Kocsis, B., Haiman, Z., & Márka, S. 2017b, *The Astrophysical Journal*, 835, 165, doi: [10.3847/1538-4357/835/2/165](https://doi.org/10.3847/1538-4357/835/2/165)
- Bellm, E. C., & Sesar, B. 2016, *pyraf-dbsp: Reduction pipeline for the Palomar Double Beam Spectrograph*. <http://ascl.net/1602.002>
- Berry, C. P. L., Mandel, I., Middleton, H., et al. 2015, *The Astrophysical Journal*, 804, 114, doi: [10.1088/0004-637x/804/2/114](https://doi.org/10.1088/0004-637x/804/2/114)
- Bertin, E. 2006, in *Astronomical Society of the Pacific Conference Series*, Vol. 351, *Astronomical Data Analysis Software and Systems XV*, ed. C. Gabriel, C. Arviset, D. Ponz, & S. Enrique, 112
- Bertin, E., & Arnouts, S. 1996, *Astronomy and Astrophysics Supplement Series*, 117, 393, doi: [10.1051/aas:1996164](https://doi.org/10.1051/aas:1996164)
- Bertin, E., & Arnouts, S. 1996, *A&AS*, 117, 393, doi: [10.1051/aas:1996164](https://doi.org/10.1051/aas:1996164)
- Bertin, E., Mellier, Y., Radovich, M., et al. 2002, *Astronomical Data Analysis Software and Systems XI*, 281, 228
- Bertin, E., Mellier, Y., Radovich, M., et al. 2002, in *Astronomical Society of the Pacific Conference Series*, Vol. 281, *Astronomical Data Analysis Software and Systems XI*, ed. D. A. Bohlender, D. Durand, & T. H. Handley, 228
- Bessell, M. S. 1990, *Publications of the Astronomical Society of the Pacific*, 102, 1181, doi: [10.1086/132749](https://doi.org/10.1086/132749)
- Blanton, M. R., & Roweis, S. 2007, *AJ*, 133, 734, doi: [10.1086/510127](https://doi.org/10.1086/510127)
- Bom, C. R., & Palmese, A. 2023, *Standard Siren Cosmology with Gravitational Waves from Binary Black Hole Mergers in Active Galaxy Nuclei*, arXiv, doi: [10.48550/arXiv.2307.01330](https://doi.org/10.48550/arXiv.2307.01330)
- Boone, K. 2021, *The Astronomical Journal*, 162, 275, doi: [10.3847/1538-3881/ac2a2d](https://doi.org/10.3847/1538-3881/ac2a2d)
- Buckley, D. A. H., Swart, G. P., & Meiring, J. G. 2006, *Ground-based and Airborne Telescopes*, 6267, 62670Z, doi: [10.1117/12.673750](https://doi.org/10.1117/12.673750)
- Burgh, E. B., Nordsieck, K. H., Kobulnicky, H. A., et al. 2003, *Instrument Design and Performance for Optical/Infrared Ground-based Telescopes*, 4841, 1463, doi: [10.1117/12.460312](https://doi.org/10.1117/12.460312)
- Burrows, D. N., Hill, J. E., Nousek, J. A., et al. 2005, *Space Science Reviews*, 120, 165, doi: [10.1007/s11214-005-5097-2](https://doi.org/10.1007/s11214-005-5097-2)
- Cabrera, T., Hu, L., Andreoni, I., et al. 2023, *GRB Coordinates Network*, 34763, 1
- Cappellari, M. 2023, *MNRAS*, 526, 3273, doi: [10.1093/mnras/stad2597](https://doi.org/10.1093/mnras/stad2597)
- Chen, H.-Y., Fishbach, M., & Holz, D. E. 2018, *Nature*, 562, 545, doi: [10.1038/s41586-018-0606-0](https://doi.org/10.1038/s41586-018-0606-0)
- Chornock, R., Berger, E., Kasen, D., et al. 2017, *ApJL*, 848, L19, doi: [10.3847/2041-8213/aa905c](https://doi.org/10.3847/2041-8213/aa905c)

- Clark, P., Graur, O., Callow, J., et al. 2024, *Monthly Notices of the Royal Astronomical Society*, 528, 7076, doi: [10.1093/mnras/stae460](https://doi.org/10.1093/mnras/stae460)
- Cook, D. O., Mazzarella, J. M., Helou, G., et al. 2023, *Completeness of the NASA/IPAC Extragalactic Database (NED) – Local Volume Sample*. <https://arxiv.org/abs/2306.06271>
- Coughlin, M. W., Tao, D., Chan, M. L., et al. 2018, *Monthly Notices of the Royal Astronomical Society*, 478, 692, doi: [10.1093/mnras/sty1066](https://doi.org/10.1093/mnras/sty1066)
- Coughlin, M. W., Bloom, J. S., Nir, G., et al. 2023, *A Data Science Platform to Enable Time-Domain Astronomy*, arXiv, doi: [10.48550/arXiv.2305.00108](https://doi.org/10.48550/arXiv.2305.00108)
- Coulter, D. A., Foley, R. J., Kilpatrick, C. D., et al. 2017, *Science*, 358, 1556, doi: [10.1126/science.aap9811](https://doi.org/10.1126/science.aap9811)
- DESI Collaboration, Adame, A. G., Aguilar, J., et al. 2023, arXiv e-prints, arXiv:2306.06308, doi: [10.48550/arXiv.2306.06308](https://doi.org/10.48550/arXiv.2306.06308)
- Dey, A., Schlegel, D. J., Lang, D., et al. 2019, *AJ*, 157, 168, doi: [10.3847/1538-3881/ab089d](https://doi.org/10.3847/1538-3881/ab089d)
- Dittmann, A. J., Dempsey, A. M., & Li, H. 2024, *ApJ*, 964, 61, doi: [10.3847/1538-4357/ad23ce](https://doi.org/10.3847/1538-4357/ad23ce)
- Drout, M. R., Piro, A. L., Shappee, B. J., et al. 2017, *Science*, 358, 1570, doi: [10.1126/science.aaq0049](https://doi.org/10.1126/science.aaq0049)
- Duras, F., Bongiorno, A., Ricci, F., et al. 2020, *Astronomy and Astrophysics*, 636, A73, doi: [10.1051/0004-6361/201936817](https://doi.org/10.1051/0004-6361/201936817)
- Evans, P. A., Page, K. L., Beardmore, A. P., et al. 2023, *MNRAS*, 518, 174, doi: [10.1093/mnras/stac2937](https://doi.org/10.1093/mnras/stac2937)
- Evans, P. A., Beardmore, A. P., Page, K. L., et al. 2009, *MNRAS*, 397, 1177, doi: [10.1111/j.1365-2966.2009.14913.x](https://doi.org/10.1111/j.1365-2966.2009.14913.x)
- Evans, P. A., Cenko, S. B., Kennea, J. A., et al. 2017, *Science*, 358, 1565, doi: [10.1126/science.aap9580](https://doi.org/10.1126/science.aap9580)
- Finn, L. S., & Chernoff, D. F. 1993, *Physical Review D*, 47, 2198–2219, doi: [10.1103/physrevd.47.2198](https://doi.org/10.1103/physrevd.47.2198)
- Flaugher, B., Diehl, H. T., Honscheid, K., et al. 2015, *The Astronomical Journal*, 150, 150, doi: [10.1088/0004-6256/150/5/150](https://doi.org/10.1088/0004-6256/150/5/150)
- Flesch, E. W. 2023, *The Million Quasars (Milliquas) Catalogue*, V8, arXiv, doi: [10.48550/arXiv.2308.01505](https://doi.org/10.48550/arXiv.2308.01505)
- Flewelling, H. A., Magnier, E. A., Chambers, K. C., et al. 2020, *The Astrophysical Journal Supplement Series*, 251, 7, doi: [10.3847/1538-4365/abb82d](https://doi.org/10.3847/1538-4365/abb82d)
- Gaia Collaboration, Prusti, T., de Bruijne, J. H. J., et al. 2016, *Astronomy and Astrophysics*, 595, A1, doi: [10.1051/0004-6361/201629272](https://doi.org/10.1051/0004-6361/201629272)
- Gaia Collaboration, Brown, A. G. A., Vallenari, A., et al. 2021, *A&A*, 649, A1, doi: [10.1051/0004-6361/202039657](https://doi.org/10.1051/0004-6361/202039657)
- Garcia, A., Morgan, R., Herner, K., et al. 2020, *The Astrophysical Journal*, 903, 75, doi: [10.3847/1538-4357/abb823](https://doi.org/10.3847/1538-4357/abb823)
- Gayathri, V., Yang, Y., Tagawa, H., Haiman, Z., & Bartos, I. 2021, *The Astrophysical Journal Letters*, 920, L42, doi: [10.3847/2041-8213/ac2cc1](https://doi.org/10.3847/2041-8213/ac2cc1)
- Gehrels, N., Chincarini, G., Giommi, P., et al. 2004, *The Astrophysical Journal*, 611, 1005, doi: [10.1086/422091](https://doi.org/10.1086/422091)
- Goldstein, A., Veres, P., Burns, E., et al. 2017, *ApJL*, 848, L14, doi: [10.3847/2041-8213/aa8f41](https://doi.org/10.3847/2041-8213/aa8f41)
- Goldstein, D. A., Andreoni, I., Nugent, P. E., et al. 2019, *The Astrophysical Journal*, 881, L7, doi: [10.3847/2041-8213/ab3046](https://doi.org/10.3847/2041-8213/ab3046)
- Górski, K. M., Hivon, E., Banday, A. J., et al. 2005, *The Astrophysical Journal*, 622, 759, doi: [10.1086/427976](https://doi.org/10.1086/427976)
- Gössl, C. A., & Riffeser, A. 2002, *A&A*, 381, 1095, doi: [10.1051/0004-6361:20011522](https://doi.org/10.1051/0004-6361:20011522)
- Graham, M. J., Ford, K. E. S., McKernan, B., et al. 2020, *Physical Review Letters*, 124, 251102, doi: [10.1103/PhysRevLett.124.251102](https://doi.org/10.1103/PhysRevLett.124.251102)
- Graham, M. J., McKernan, B., Ford, K. E. S., et al. 2023, *The Astrophysical Journal*, 942, 99, doi: [10.3847/1538-4357/aca480](https://doi.org/10.3847/1538-4357/aca480)
- Green, G. M. 2018, *Journal of Open Source Software*, 3, 695, doi: [10.21105/joss.00695](https://doi.org/10.21105/joss.00695)
- Greene, J. E., & Ho, L. C. 2005, *ApJ*, 630, 122, doi: [10.1086/431897](https://doi.org/10.1086/431897)
- Greene, J. E., & Ho, L. C. 2007, *Astrophys. J.*, 667, 131, doi: [10.1088/0004-637X/704/2/1743](https://doi.org/10.1088/0004-637X/704/2/1743)
- Guo, H., Shen, Y., & Wang, S. 2018, *PyQSOFit: Python code to fit the spectrum of quasars*, *Astrophysics Source Code Library*. <http://ascl.net/1809.008>
- Harris, C. R., Millman, K. J., van der Walt, S. J., et al. 2020, *Nature*, 585, 357, doi: [10.1038/s41586-020-2649-2](https://doi.org/10.1038/s41586-020-2649-2)
- Herner, K., Annis, J., Brout, D., et al. 2020, *Astronomy and Computing*, 33, 100425, doi: [10.1016/j.ascom.2020.100425](https://doi.org/10.1016/j.ascom.2020.100425)
- Hilton, M., Hasselfield, M., Sifón, C., et al. 2018, *ApJS*, 235, 20, doi: [10.3847/1538-4365/aaa6cb](https://doi.org/10.3847/1538-4365/aaa6cb)
- Holz, D. E., & Hughes, S. A. 2005, *The Astrophysical Journal*, 629, 15, doi: [10.1086/431341](https://doi.org/10.1086/431341)
- Hopp, U., Bender, R., Grupp, F., et al. 2014, in *Society of Photo-Optical Instrumentation Engineers (SPIE) Conference Series*, Vol. 9145, *Ground-based and Airborne Telescopes V*, ed. L. M. Stepp, R. Gilmozzi, & H. J. Hall, 91452D, doi: [10.1117/12.2054498](https://doi.org/10.1117/12.2054498)
- Hotokezaka, K., Nakar, E., Gottlieb, O., et al. 2019, *Nature Astronomy*, 3, 940, doi: [10.1038/s41550-019-0820-1](https://doi.org/10.1038/s41550-019-0820-1)
- Hu, L., Cabrera, T., Palmese, A., et al. 2024, in prep.

- Hu, L., Wang, L., Chen, X., & Yang, J. 2022, *The Astrophysical Journal*, 936, 157, doi: [10.3847/1538-4357/ac7394](https://doi.org/10.3847/1538-4357/ac7394)
- Hunter, J. D. 2007, *Computing in Science & Engineering*, 9, 90, doi: [10.1109/MCSE.2007.55](https://doi.org/10.1109/MCSE.2007.55)
- Ivezić, Ž., Kahn, S. M., Tyson, J. A., et al. 2019, *The Astrophysical Journal*, 873, 111, doi: [10.3847/1538-4357/ab042c](https://doi.org/10.3847/1538-4357/ab042c)
- Kasliwal, M., Nakar, E., Singer, L., et al. 2017, *Science*, 358, 1559
- Kauffmann, G., Heckman, T. M., Tremonti, C., et al. 2003, *MNRAS*, 346, 1055, doi: [10.1111/j.1365-2966.2003.07154.x](https://doi.org/10.1111/j.1365-2966.2003.07154.x)
- Kessler, R., Narayan, G., Avelino, A., et al. 2019, *Publications of the Astronomical Society of the Pacific*, 131, 094501, doi: [10.1088/1538-3873/ab26f1](https://doi.org/10.1088/1538-3873/ab26f1)
- Kewley, L. J., Dopita, M. A., Sutherland, R. S., Heisler, C. A., & Trevena, J. 2001, *ApJ*, 556, 121, doi: [10.1086/321545](https://doi.org/10.1086/321545)
- Kewley, L. J., Groves, B., Kauffmann, G., & Heckman, T. 2006, *MNRAS*, 372, 961, doi: [10.1111/j.1365-2966.2006.10859.x](https://doi.org/10.1111/j.1365-2966.2006.10859.x)
- Klimenko, S., Vedovato, G., Drago, M., et al. 2016, *Physical Review D*, 93, doi: [10.1103/physrevd.93.042004](https://doi.org/10.1103/physrevd.93.042004)
- Kobulnicky, H. A., Nordsieck, K. H., Burgh, E. B., et al. 2003, *Instrument Design and Performance for Optical/Infrared Ground-based Telescopes*, 4841, 1634, doi: [10.1117/12.460315](https://doi.org/10.1117/12.460315)
- Labrie, K., Anderson, K., Cárdenes, R., Simpson, C., & Turner, J. E. H. 2019, *ASP Conference Series*, 523, 321
- Lang-Bardl, F., Bender, R., Goessl, C., et al. 2016, in *Society of Photo-Optical Instrumentation Engineers (SPIE) Conference Series*, Vol. 9908, *Ground-based and Airborne Instrumentation for Astronomy VI*, ed. C. J. Evans, L. Simard, & H. Takami, 990844, doi: [10.1117/12.2232039](https://doi.org/10.1117/12.2232039)
- Ligo Scientific Collaboration, VIRGO Collaboration, & Kagra Collaboration. 2023a, *GRB Coordinates Network*, 34757, 1
- . 2023b, *GRB Coordinates Network*, 34758, 1
- . 2023c, *GRB Coordinates Network*, 34758, 1
- Lipunov, V. M., Gorbovskoy, E., Kornilov, V. G., et al. 2017, *ApJL*, 850, L1, doi: [10.3847/2041-8213/aa92c0](https://doi.org/10.3847/2041-8213/aa92c0)
- Magnier, E. A., Schlafly, E., Finkbeiner, D., et al. 2013, *ApJS*, 205, 20, doi: [10.1088/0067-0049/205/2/20](https://doi.org/10.1088/0067-0049/205/2/20)
- Mainzer, A., Grav, T., Bauer, J., et al. 2011, *ApJ*, 743, 156, doi: [10.1088/0004-637X/743/2/156](https://doi.org/10.1088/0004-637X/743/2/156)
- Mainzer, A., Bauer, J., Cutri, R. M., et al. 2014, *ApJ*, 792, 30, doi: [10.1088/0004-637X/792/1/30](https://doi.org/10.1088/0004-637X/792/1/30)
- Margutti, R., Berger, E., Fong, W., et al. 2017, *ApJL*, 848, L20, doi: [10.3847/2041-8213/aa9057](https://doi.org/10.3847/2041-8213/aa9057)
- McKernan, B., & Ford, K. E. S. 2024, *MNRAS*, 531, 3479, doi: [10.1093/mnras/stae1351](https://doi.org/10.1093/mnras/stae1351)
- McKernan, B., Ford, K. E. S., Bartos, I., et al. 2019, *The Astrophysical Journal*, 884, L50, doi: [10.3847/2041-8213/ab4886](https://doi.org/10.3847/2041-8213/ab4886)
- McKinney, W. 2010, *Proceedings of the 9th Python in Science Conference*, 56, doi: [10.25080/Majora-92bf1922-00a](https://doi.org/10.25080/Majora-92bf1922-00a)
- McManus, S., & Olsen, K. 2021, *The NOIRLab Mirror*, 2, 33
- Messick, C., Blackburn, K., Brady, P., et al. 2017, *Physical Review D*, 95, doi: [10.1103/physrevd.95.042001](https://doi.org/10.1103/physrevd.95.042001)
- Morgan, R., Soares-Santos, M., Annis, J., et al. 2020, *The Astrophysical Journal*, 901, 83, doi: [10.3847/1538-4357/abafaa](https://doi.org/10.3847/1538-4357/abafaa)
- Nicholl, M., Berger, E., Kasen, D., et al. 2017, *ApJL*, 848, L18, doi: [10.3847/2041-8213/aa9029](https://doi.org/10.3847/2041-8213/aa9029)
- Onken, C. A., Wolf, C., Bessell, M. S., et al. 2024, *SkyMapper Southern Survey: Data Release 4*. <https://arxiv.org/abs/2402.02015>
- Palmese, A., Fishbach, M., Burke, C. J., Annis, J., & Liu, X. 2021, *The Astrophysical Journal*, 914, L34, doi: [10.3847/2041-8213/ac0883](https://doi.org/10.3847/2041-8213/ac0883)
- Palmese, A., Kaur, R., Hajela, A., et al. 2024, *Physical Review D*, 109, 063508
- Perley, D. A. 2019, *PASP*, 131, 084503, doi: [10.1088/1538-3873/ab215d](https://doi.org/10.1088/1538-3873/ab215d)
- Perna, R., Lazzati, D., & Cantiello, M. 2021, *ApJL*, 906, L7, doi: [10.3847/2041-8213/abd319](https://doi.org/10.3847/2041-8213/abd319)
- Pian, E., D’Avanzo, P., Benetti, S., et al. 2017, *Nature*, 551, 67, doi: [10.1038/nature24298](https://doi.org/10.1038/nature24298)
- Rousselot, P., Lidman, C., Cuby, J. G., Moreels, G., & Monnet, G. 2000, *Astronomy and Astrophysics*, 354, 1134
- Sachdev, S., Caudill, S., Fong, H., et al. 2019, *The GstLAL Search Analysis Methods for Compact Binary Mergers in Advanced LIGO’s Second and Advanced Virgo’s First Observing Runs*. <https://arxiv.org/abs/1901.08580>
- Savchenko, V., Ferrigno, C., Kuulkers, E., et al. 2017, *ApJL*, 848, L15, doi: [10.3847/2041-8213/aa8f94](https://doi.org/10.3847/2041-8213/aa8f94)
- Schlafly, E. F., & Finkbeiner, D. P. 2011, *The Astrophysical Journal*, 737, 103, doi: [10.1088/0004-637X/737/2/103](https://doi.org/10.1088/0004-637X/737/2/103)
- Schutz, B. F. 1986, *Nature*, 323, 310, doi: [10.1038/323310a0](https://doi.org/10.1038/323310a0)
- Shappee, B. J., Simon, J. D., Drout, M. R., et al. 2017, *Science*, 358, 1574, doi: [10.1126/science.aag0186](https://doi.org/10.1126/science.aag0186)
- Singer, L. P., Chen, H.-Y., Holz, D. E., et al. 2016, *The Astrophysical Journal*, 829, L15, doi: [10.3847/2041-8205/829/1/L15](https://doi.org/10.3847/2041-8205/829/1/L15)

- Sirko, E., & Goodman, J. 2003, *MNRAS*, 341, 501, doi: [10.1046/j.1365-8711.2003.06431.x](https://doi.org/10.1046/j.1365-8711.2003.06431.x)
- Skrutskie, M. F., Cutri, R. M., Stiening, R., et al. 2006, *AJ*, 131, 1163, doi: [10.1086/498708](https://doi.org/10.1086/498708)
- Smartt, S. J., Chen, T. W., Jerkstrand, A., et al. 2017, *Nature*, 551, 75, doi: [10.1038/nature24303](https://doi.org/10.1038/nature24303)
- Soares-Santos, M., Kessler, R., Berger, E., et al. 2016, *The Astrophysical Journal Letters*, 823, L33, doi: [10.3847/2041-8205/823/2/L33](https://doi.org/10.3847/2041-8205/823/2/L33)
- Soares-Santos, M., Holz, D. E., Annis, J., et al. 2017, *The Astrophysical Journal*, 848, L16, doi: [10.3847/2041-8213/aa9059](https://doi.org/10.3847/2041-8213/aa9059)
- Storey-Fisher, K., Hogg, D. W., Rix, H.-W., et al. 2024, *The Astrophysical Journal*, 964, 69, doi: [10.3847/1538-4357/ad1328](https://doi.org/10.3847/1538-4357/ad1328)
- Symbalisty, E., & Schramm, D. N. 1982, *Astrophysical Letters*, 22, 143
- Tagawa, H., Kimura, S. S., Haiman, Z., Perna, R., & Bartos, I. 2023, *ApJ*, 950, 13, doi: [10.3847/1538-4357/acc4bb](https://doi.org/10.3847/1538-4357/acc4bb)
- Tagawa, H., Kimura, S. S., Haiman, Z., Perna, R., & Bartos, I. 2024, *Astrophys. J.*, 966, 21, doi: [10.3847/1538-4357/ad2e0b](https://doi.org/10.3847/1538-4357/ad2e0b)
- Tanvir, N. R., Levan, A. J., González-Fernández, C., et al. 2017, *ApJL*, 848, L27, doi: [10.3847/2041-8213/aa90b6](https://doi.org/10.3847/2041-8213/aa90b6)
- Thompson, T. A., Quataert, E., & Murray, N. 2005, *ApJ*, 630, 167, doi: [10.1086/431923](https://doi.org/10.1086/431923)
- Troja, E., Piro, L., Van Eerten, H., et al. 2017, *Nature*, 551, 71
- Utsumi, Y., Tanaka, M., Tominaga, N., et al. 2017, *PASJ*, 69, 101, doi: [10.1093/pasj/psx118](https://doi.org/10.1093/pasj/psx118)
- Valdes, F., Gruendl, R., & DES Project. 2014, in *Astronomical Society of the Pacific Conference Series*, Vol. 485, *Astronomical Society of the Pacific Conference Series*, ed. N. Manset & P. Forshay, 379
- Valenti, S., Sand, D. J., Yang, S., et al. 2017, *ApJL*, 848, L24, doi: [10.3847/2041-8213/aa8edf](https://doi.org/10.3847/2041-8213/aa8edf)
- van der Walt, S. J., Crellin-Quick, A., & Bloom, J. S. 2019, *Journal of Open Source Software*, 4, doi: [10.21105/joss.01247](https://doi.org/10.21105/joss.01247)
- Varma, V., Biscoveanu, S., Islam, T., et al. 2022, *PhRvL*, 128, 191102, doi: [10.1103/PhysRevLett.128.191102](https://doi.org/10.1103/PhysRevLett.128.191102)
- Vazdekis, A., Koleva, M., Ricciardelli, E., Röck, B., & Falcón-Barroso, J. 2016, *MNRAS*, 463, 3409, doi: [10.1093/mnras/stw2231](https://doi.org/10.1093/mnras/stw2231)
- Wang, Y.-H., Lazzati, D., & Perna, R. 2022, *Monthly Notices of the Royal Astronomical Society*, 516, 5935–5944, doi: [10.1093/mnras/stac1968](https://doi.org/10.1093/mnras/stac1968)
- Wright, E. L., Eisenhardt, P. R. M., Mainzer, A. K., et al. 2010a, *The Astronomical Journal*, 140, 1868, doi: [10.1088/0004-6256/140/6/1868](https://doi.org/10.1088/0004-6256/140/6/1868)
- . 2010b, *The Astronomical Journal*, 140, 1868, doi: [10.1088/0004-6256/140/6/1868](https://doi.org/10.1088/0004-6256/140/6/1868)
- Wyatt, S. D., Tohuvavohu, A., Arcavi, I., et al. 2020, *The Astrophysical Journal*, 894, 127, doi: [10.3847/1538-4357/ab855e](https://doi.org/10.3847/1538-4357/ab855e)
- Zonca, A., Singer, L., Lenz, D., et al. 2019, *The Journal of Open Source Software*, 4, 1298, doi: [10.21105/joss.01298](https://doi.org/10.21105/joss.01298)